

# REPORT DOCUMENTATION PAGE

Form Approved  
OMB No. 0704-0188

Public reporting burden for this collection of information is estimated to average 1 hour per response, including the time for reviewing instructions, searching existing data sources, gathering and maintaining the data needed, and completing and reviewing the collection of information. Send comments regarding this burden estimate or any other aspect of this collection of information, including suggestions for reducing this burden, to Washington Headquarters Services, Directorate for Information Operations and Reports, 1215 Jefferson Davis Highway, Suite 1204, Arlington, VA 22202-4302, and to the Office of Management and Budget, Paperwork Reduction Project (0704-0188), Washington, DC 20503.

1. AGENCY USE ONLY (Leave blank)		2. REPORT DATE 6 July 1998		3. REPORT TYPE AND DATES COVERED Final Technical Report 1 Feb 95 to 31 Jan 98	
4. TITLE AND SUBTITLE Characterizing Scale Dependent Hydraulic Properties with Measurement of Dielectric Properties				5. FUNDING NUMBERS F49620-95-1-0166	
6. AUTHOR(S) Assoc Professor Rosemary Knight					
7. PERFORMING ORGANIZATION NAME(S) AND ADDRESS(ES) Dept of Earth and Ocean Sciences University of British Columbia 2219 Main Mall Vancouver, B.C. Canada V6T 1Z4				8. PERFORMING ORGANIZATION REPORT NUMBER	
9. SPONSORING/MONITORING AGENCY NAME(S) AND ADDRESS(ES) AFOSR/NA 110 Duncan Avenue, Suite B115 Bolling AFB, DC 20332-8050				10. SPONSORING/MONITORING AGENCY REPORT NUMBER  F49620-95-1-0166	
11. SUPPLEMENTARY NOTES					
12a. DISTRIBUTION AVAILABILITY STATEMENT Approved for public release; distribution unlimited.				12b. DISTRIBUTION CODE	
13. ABSTRACT (Maximum 200 words) The objective of this research project was to develop ways to obtain information about the hydraulic properties of the subsurface from measurement of dielectric properties. The focus of the research was the use of ground penetrating radar (GPR), a high resolution geophysical technique that images changes in dielectric properties of the subsurface. Geostatistical analysis of GPR images was found to provide a non-invasive means of characterizing the spatial heterogeneity of the subsurface. Results from a field experiment, which involved the collection of GPR data across a cliff face, showed that the spatial variability seen in the GPR image was representative of the spatial variability seen in the grain size of the sediments in the cliff. Dielectric measurements can be used to obtain estimates of the magnitude of hydraulic properties, if the relationship between dielectric properties and hydraulic properties is known. Theoretical and numerical modeling, and laboratory measurements on layered materials investigated the effect of layer thickness and frequency or wavelength of the measurement. By taking these parameters into account the accuracy with which hydraulic properties are obtained from dielectric measurements can be significantly improved.					
14. SUBJECT TERMS  radar, dielectric, geostatistics, hydrogeology				15. NUMBER OF PAGES 61	
				16. PRICE CODE	
17. SECURITY CLASSIFICATION OF REPORT  Unclassified	18. SECURITY CLASSIFICATION OF THIS PAGE  Unclassified	19. SECURITY CLASSIFICATION OF ABSTRACT  Unclassified	20. LIMITATION OF ABSTRACT  UL		

## Table of Contents

<b>Executive Summary.....</b>	<b>1</b>
<b>1 Introduction.....</b>	<b>6</b>
<b>2 Geostatistical Analysis of Ground Penetrating Radar Data: A Means of Characterizing the Heterogeneity of the Subsurface.....</b>	<b>8</b>
Introduction.....	8
Classification of Radar Units.....	9
Method of Geostatistical Analysis.....	10
Calibration Field Experiment.....	19
Analysis of GPR Data From Selected Depositional Environments.....	20
Conclusions.....	33
<b>3 The Relationship Between Dielectric Constant and Hydraulic Properties.....</b>	<b>34</b>
Introduction.....	34
Theoretical Study of Properties of Layered Materials.....	36
Introduction.....	36
Description of Models and Theories.....	36
Data/Results and Discussion.....	38
Conclusions.....	41
Numerical Modeling of EM Wave Propagation in Layered Systems.....	41
Introduction.....	41
Method of Numerical Analysis.....	42
Data/Results.....	45
Conclusions.....	47
Laboratory Measurements.....	49
Introduction/Experimental Methods.....	49
Data Collection and Results.....	50
Conclusions.....	52
Conclusions.....	52
<b>4 Electrical Conductivity Estimates from GPR Data.....</b>	<b>53</b>
<b>5 Conclusions and Recommendations.....</b>	<b>55</b>
<b>References.....</b>	<b>58</b>
<b>Appendix A - bound separately</b>	

## EXECUTIVE SUMMARY

A critical step in modeling groundwater flow and/or contaminant transport at a site is to obtain an accurate 3-D model of the hydraulic conductivity of the subsurface. Past practice has often involved assigning average values of hydraulic conductivity  $K$  to simple layered models of the subsurface. However it is now widely recognized that using averaged values of  $K$  is insufficient; the spatial variability in  $K$ , the natural heterogeneity of the subsurface, has a significant effect on groundwater flow and is an important parameter in modeling contaminant transport. The challenge is to develop methods that can be used to accurately, and cost-effectively characterize the subsurface in terms of its hydraulic properties. Information is needed about both the magnitude and the spatial variability in properties. We have investigated the use of measurement of dielectric properties as a means of obtaining both these types of information.

A central goal of our research is to develop an understanding of the link between dielectric properties and hydraulic properties of the subsurface. Measurements of dielectric properties of the subsurface can be obtained non-invasively from ground penetrating radar data. The dielectric constant of a volume of the subsurface controls the velocity of the electromagnetic wave; changes in the dielectric constant of the subsurface determine the magnitude of the reflections seen in GPR data. In this way a "map" of the dielectric constant of the subsurface can be obtained from GPR data. From an applied perspective our research can be described as addressing the question: How can we use these measurements of dielectric constant to characterize hydraulic conductivity at a site? Our approach is a combination of field experiments, laboratory experiments, and theoretical modeling.

One focus of our research has been to work with GPR data and to develop data analysis methods that allow us to extract information about the spatial variability in hydraulic properties. Specifically we have assessed and developed the use of geostatistical methods to quantify the heterogeneity and

19981016 021

structure seen in the GPR image; our hypothesis being that this gives us a valid description of the heterogeneity of hydraulic properties of the subsurface. We analyze the GPR data by constructing an experimental variogram, where our parameter of interest is the amplitude of the reflectors in the GPR data, and then fit the experimental variograms with standard variogram models.

In order to determine the link between the spatial variability seen in the GPR image and the true spatial variability in hydraulic properties of the subsurface, we conducted a cliff-face experiment. In this experiment we collected GPR data across the top of the cliff and could examine and photograph the imaged sedimentary sequence, which was a package of alternating coarse-grained sand and fine-grained silt. We used a geostatistical analysis of the photograph of the cliff to quantify the spatial variability or correlation structure in grain size in the sediments. The correlation structure we obtained from the GPR image was in excellent agreement with that from the photograph indicating that the GPR image had captured information about the spatial distribution of the coarse-grained/fine-grained sequence.

In an extension of this study, experimental variograms have been obtained from GPR data from a number of different sedimentary environments. The experimental variograms are all of excellent quality, and have led us to conclude that the geostatistical analysis of GPR data does provide a way of quantifying spatial variability in a wide range of geologic settings. In addition we find indications that the correlation structure in the GPR image is related to the processes in the depositional environment, leading us to suggest that there can be characteristic GPR "signatures" associated with different environments.

We conclude that the geostatistical analysis of GPR data from a site can be used for site characterization where information is needed about the nature and extent of the spatial heterogeneity of the subsurface. We have developed an interactive computer program, included in the insert at the back of this report, that makes it possible to select and analyze regions within a GPR image, and

model the resulting variogram. This could be used with GPR data from any site as a means of planning for or integrating data obtained through drilling and direct sampling.

The second aspect of our research has involved a study of the direct relationship between the measured values of the dielectric constant of a volume of the subsurface and hydraulic properties. Estimates of dielectric constant can be extracted from GPR data and can also be obtained through the use of time domain reflectometry. These estimates of dielectric constant can then be used to estimate hydraulic properties through the use of relationships between dielectric and hydraulic properties. While previous research has addressed these relationships for homogeneous materials, we have extended this work to consider the relationship between these properties in heterogeneous materials. We have considered a specific form of heterogeneity, layering, which is very likely to be encountered in measurements of the subsurface.

Theoretical modeling of the relationship between measured dielectric constant and water content has demonstrated the errors that can result if the sample size and contained heterogeneity, such as layering, are not taken into account. In modeling the measured dielectric constant, the critical parameter is the thickness of the layers relative to the wavelength of the measurement. In one limit, where the wavelength is less than the layer thickness, ray theory is a valid description of the electromagnetic response of the material; in the other limit, where the wavelength is greater than the layer thickness, an effective medium approximation must be used. The errors that result from simply assuming a homogeneous system become pronounced due to the saturation heterogeneity that can develop.

In addition to theoretical and numerical modeling of electromagnetic wave propagation in layered materials, laboratory measurements of a sand/silt system have been conducted. In these experimental results we can see very clearly the predicted transition from ray theory to effective medium theory. The results show the complex nature of the relationship between dielectric

properties and hydraulic properties in heterogeneous materials, and highlight the need to ensure that there is a valid theoretical basis for the relationship that is used to extract hydraulic information from dielectric measurements.

In the use of dielectric measurements for subsurface characterization, the level of accuracy in interpretation of the dielectric data can be significantly improved if additional parameters are measured. A methodology has been developed that allows us to extract electrical conductivity from GPR data; knowledge of electrical conductivity can assist in constraining the interpretation of the GPR data in terms of hydraulic properties of the subsurface. Given that this requires the collection of no additional data, we conclude that estimates of electrical conductivity could be easily obtained at a site to improve the use of GPR to estimate subsurface hydraulic properties.

This research has significantly advanced our understanding of how best to use dielectric measurements, from GPR data, to both estimate the magnitude of hydraulic properties and to characterize spatial heterogeneity; both important aspects of site characterization. While much of this research has involved the study of fundamental scientific issues, some of the results of the research can be readily applied, now, to site characterization problems. In particular we highly recommend that geostatistical analysis of GPR images be used as a means of obtaining information about the nature and extent of spatial heterogeneity in the subsurface.

This report describes all aspects of our three-year project. Additional and more detailed information can be found in the following publications and presentations that resulted from this project:

#### **Refereed Publications:**

- Rea, J., and Knight, R., Geostatistical analysis of ground penetrating radar data: A means of describing spatial variation in the subsurface, Water Resources Research, 34, 329-339, 1998.
- Rea, J., and Knight, R., Characterization of the Brookwood aquifer using ground penetrating radar, *in* Geological Survey of Canada Bulletin: Aquifer Delineation, Fraser Lowlands and Delta, B.C.: Mapping, Geophysics, and Groundwater Modelling, B.D. Ricketts (ed.), in press, 1998.

- Rea, J., and Knight, R., Obtaining estimates of electrical conductivity from the attenuation in ground penetrating radar data, submitted to Geophysics September 1997, in revision.
- Chan, C. Y., and Knight, R. J., Determining water content and saturation from dielectric measurements of layered materials, submitted to Water Resources Research, 1998.

#### **Theses:**

- Rea, J., Ground Penetrating Radar Applications in Hydrology, Ph.D. dissertation, University of British Columbia, 88 pages, 1996.
- Chan, C. Y., Dielectric Properties of Layered Materials, Ph.D. dissertation, University of British Columbia, in preparation.

#### **Other Publications/Presentations:**

- Rea, J., and Knight, R.J., The use of ground penetrating radar for aquifer characterization: an example from southwestern British Columbia, Proceedings, Symposium for Application of Geophysics to Environmental and Engineering Problems, 23-26 April, Orlando, FL, 10 pages, 1995.
- Rea, J. and Knight, R.J., The use of ground penetrating for aquifer characterization: An example from southwestern British Columbia, Geological Assoc. of Canada - Mineralogical Assoc. of Canada Meeting, Victoria, May 1995.
- Rea, J., and Knight, R.J., Ground penetrating radar applications for determining hydrologic length scales in aquifer environments, Canadian Geophysical Union, Banff, Alta., May 1996.
- Chan, C.Y., and Knight, R., Rock Properties of Layered Sand and Clay, presented at Scientific Meeting of the Canadian Geophysical Union, Banff, Canada, May 5-11, 1995.
- Rea, J., and Knight, R.J., The use of ground penetrating radar for aquifer characterization: a geostatistical approach, Extended Abstracts, SEG Annual Meeting, Denver, CO, 1996.
- Chan, C. and Knight, R.J., Dielectric properties of layered systems, EOS Transactions, American Geophysical Union, v. 77, 1996.
- Knight, R.J., Rea, J., and Tercier, P., Geostatistical analysis of ground penetrating radar data: a means of characterizing the correlation structure of sedimentary units, EOS Transactions, American Geophysical Union, v. 77, 1996.
- Knight, R., Tercier, P., Rea, J., The use of ground penetrating radar data in developing hydrogeologic models of the subsurface, Proceedings of Workshop on High Resolution Geophysics, University of Arizona, January 1997.
- Chan, C., and Knight, R., The transition zone between effective medium theory and ray theory, Extended Abstracts, Soc. of Exploration Geophysicists 67th Annual Meeting, Dallas, TX, 1997.
- Knight, R., Tercier, P., and Jol, H., The role of ground penetrating radar and geostatistics in reservoir description, The Leading Edge, 1997.
- Knight, R., Tercier, P., Rea, J., Scullard, C., Jol, H., Geostatistical analysis of ground penetrating radar data, abstract, Hazardous Substance Research Conference, May 19-21, Snowbird Utah, 1998.

The completed thesis by Jane Rea is included as Appendix A. The personnel supported by this project over three years were: Paulette Tercier (Research Scientist), Jane Rea (graduate student), Christina Chan (graduate student), Pnina Miller (graduate student), and Christian Scullard (undergraduate research assistant).



## 1

**INTRODUCTION**

A critical step in modeling groundwater flow and/or contaminant transport at a site is to obtain an accurate 3-D model of the hydraulic conductivity of the subsurface. Past practice has often involved assigning average values of hydraulic conductivity  $K$  to simple layered models of the subsurface. However it is now widely recognized that using averaged values of  $K$  is insufficient; the spatial variability in  $K$ , the natural heterogeneity of the subsurface, has a significant effect on groundwater flow and is an important parameter in modeling contaminant transport.

Of interest in this study has been the use of measurements of dielectric properties of the subsurface to characterize the spatial variability in hydraulic properties of the subsurface. Measurements of in situ dielectric properties can be made using a ground penetrating radar (GPR) system. GPR provides us with an image of the subsurface, which is actually an image of the dielectric properties of the subsurface. The GPR image is obtained by sending a pulse of electromagnetic energy into the ground and recording the amplitude of energy reflected back to the surface; energy is reflected back from interfaces across which there is a change in dielectric properties. Seen in the image is the location of interfaces, such that the GPR image is actually an image of the dielectric properties of the subsurface. One focus of our research has been to work with GPR data and to develop data analysis methods that allow us to extract information about the spatial variability in hydraulic properties. Specifically we have assessed the use of geostatistical methods to quantify the heterogeneity and structure seen in the GPR image; our hypothesis being that this gives us a valid description of the heterogeneity of hydraulic properties of the subsurface. This research is described in section 2 of this report.

The second aspect of our research, described in section 3, has involved the direct relationship between the measured values of the dielectric constant of a volume of the subsurface and hydraulic



properties. Estimates of dielectric constant can be extracted from GPR data and can also be obtained through the use of time domain reflectometry. These estimates of dielectric constant can then be used to estimate hydraulic properties through the use of relationships between dielectric and hydraulic properties. While previous research has addressed these relationship between dielectric properties and hydraulic properties for homogeneous materials, we have extended this work to consider the relationship between these properties in heterogeneous materials. We have considered a specific form of heterogeneity, layering, which is very likely to be encountered in measurements of the subsurface.

In the use of dielectric measurements for subsurface characterization, the level of accuracy in interpretation of the dielectric data can be significantly improved if additional parameters are measured. In section 4 we describe a way in which electrical conductivity can be extracted from GPR data; knowledge of electrical conductivity can assist in constraining the interpretation of the GPR data in terms of hydraulic properties of the subsurface.

As our understanding of the dielectric properties of geologic materials improves, so too does our ability to use the measurement of these properties as an effective means of subsurface characterization. We have found that measurement of dielectric properties can be used to obtain information about both the magnitude and spatial heterogeneity of hydraulic properties. The measurement of dielectric properties, by the collection of GPR data at a site, can thus provide valuable information allowing us to more accurately model the complex scale-dependent hydraulic properties of the subsurface.

## 2

## **Geostatistical Analysis of Ground Penetrating Radar Data: A Means of Characterizing the Heterogeneity of the Subsurface**

### **Introduction**

A critical step in modeling contaminant transport or remediation at a site is obtaining a realistic 3-D model of a region of the subsurface. Given the heterogeneity of the geological environment, it will never be possible to collect sufficient data through drilling and direct sampling to adequately characterize the spatial variability that exists in the subsurface. The question becomes how best to "fill in" the region between data points, or describe the region at a scale less than the scale of our sampling. A common approach is to use geostatistical methods.

Geostatistics provides a mathematical framework that can be used to describe how some property or parameter varies spatially; these spatial statistics can then be used in the development of the model of the subsurface. Some information about spatial statistics can be obtained from borehole data or cores, but due to the relatively large distances between boreholes, this usually only provides a good measure of variation in the vertical direction. To obtain a description of lateral variation data can be collected from outcrops, selected as representative of the subsurface geology, but this is extremely time consuming, and usually limited to the two dimensions of the exposed section.

We suggest that geostatistical analysis of GPR data can be used to describe the spatial variation of the subsurface. Our working hypothesis is that the links between sedimentary and hydrogeologic properties, and between sedimentary and dielectric properties, can be exploited to infer an

underlying relationship between the spatial distribution of the radar reflectors seen in a GPR section and the spatial distribution of hydrogeologic properties.

In our work we use the semivariogram, a plot which illustrates the way in which the difference between data values is related to the distance between the data values. The experimental semivariogram is described by the following equation (Deutsch and Journel, 1992):

$$\gamma(h) = \frac{1}{2N(h)} \sum_{i=1}^{N(h)} [z(x_i) - z(x_i + h)]^2 \quad (1)$$

where  $h$  is the lag, or separation vector, between two data points,  $z(x)$  and  $z(x+h)$  and  $N$  is the number of data pairs used in each summation. In general, the semivariogram function  $\gamma$  increases with increasing lag, leveling off at the "sill" when the distance between the data points becomes so large that the data values are no longer correlated. The value of the lag at this point is referred to as the range or the correlation length of the data set. In most cases a semivariogram is directional, that is, the vector  $h$  lies in a specified direction. This direction can be set to any direction of interest, but is generally that of maximum correlation. As our objective is to determine the correlation length of the radar reflectors, we use the amplitude values recorded in the radar traces as our parameter  $z$ . We obtain the experimental variogram for the GPR image and suggest that this is representative of the correlation structure of the subsurface; i.e. the GPR image provides a way of quantifying the nature of the spatial heterogeneity in the subsurface properties.

### Classification of Radar Units

An underlying assumption in the calculation of semivariograms is that the data conform to a requirement called stationarity. Stationarity means that any subset of the data will have the same

statistical description as any other subset. This is of concern in most geostatistical problems as the earth is not inherently stationary, with different geologic units displaying very different spatial variability. For the purposes of our study, this implies that we must separate, and analyze individually, data obtained from different sedimentary units.

Working with a large data set of GPR images, collected in the area of the Brookwood aquifer, southwestern British Columbia, we developed a methodology for defining "radar elements"; this is described in detail in Rea's Ph.D. thesis (appendix A) and Rea and Knight (1995). The method involves first developing a classification scheme that makes it possible to relate different regions in the GPR images to the different sedimentary or hydrogeologic units. This was done primarily using the geometry of packages of reflectors (e.g. "channel-shaped") and the length and dip of the internal reflectors (e.g. "long, subhorizontal reflectors"). Well data allowed us to relate these GPR characteristics to the different hydrogeologic units.

### **Method of Geostatistical Analysis**

In our geostatistical analysis of the GPR data, our objective is to determine the correlation length of the radar reflectors. The data values we use to construct the experimental semivariogram are the amplitude values recorded in the radar traces. We first correct for a violation of the stationarity assumption introduced by the GPR method due to the decay of amplitude down a radar trace. Uncorrected, the data at early times, having much higher amplitudes, would dominate the semivariogram calculation. We first correct the data for any time shifts due to elevation changes or problems with the electronics, then use an automatic gain control with a short window length to make the amplitudes of all the reflectors approximately equal. The high amplitude air and ground arrivals at the start of each trace are removed by simply cropping the data. A further processing step, migration of the data, might be needed to recover the true correlation length in areas with steeply dipping reflectors; migration was found to have little effect on the analysis of the data from

our study areas. As a final step before calculating a semivariogram, the radar data must be converted from a time section to a depth section so that the lag is a physical length scale. This is done using the velocity calculated from a common midpoint radar survey conducted at the site under investigation.

In our study of the geostatistical analysis of GPR data, we began by using the geostatistical software package GSLIB (Deutsch and Journel, 1992). This was however quite a tedious process. Several different FORTRAN routines from GSLIB, in a non-graphical environment, had to be used and it was only possible to compute the semivariogram in one direction. As a result we developed a program here referred to as GSWIN, a Windows 95 based program for performing geostatistical analysis on ground penetrating radar data; a copy is included on the disc submitted with this report. GSWIN is capable of displaying the variation in the semivariogram function  $\gamma$  in all directions and does so employing a graphical user interface.

GSWIN can import three types of data file formats:

1. GPR data collected and processed using Sensors and Software's PULSE EKKO GPR package. The resulting text file can then be loaded into GSWIN (Figure 2.1). A wave velocity must be specified by the user in order to determine the sampling rate in the y-direction.
2. A SCION Image (SCION Corporation, 1997) picture which has been saved in the text format. The sampling rates in the x and y directions must be entered by the user in units of metres/pixel.
3. An SGSIMM simulation. SGSIMM takes an input semivariogram and simulates a data set. This was primarily used for testing whether the program was working properly but remains part of the program as an option. A matrix size must be entered by the user to specify the size of the data set because SGSIMM outputs numbers in one column only.

Once the data are in the main window, a variogram surface can be computed. This gives the spatial variation of the data in all directions; i.e. the lag vector  $h$  can have any direction. This computation

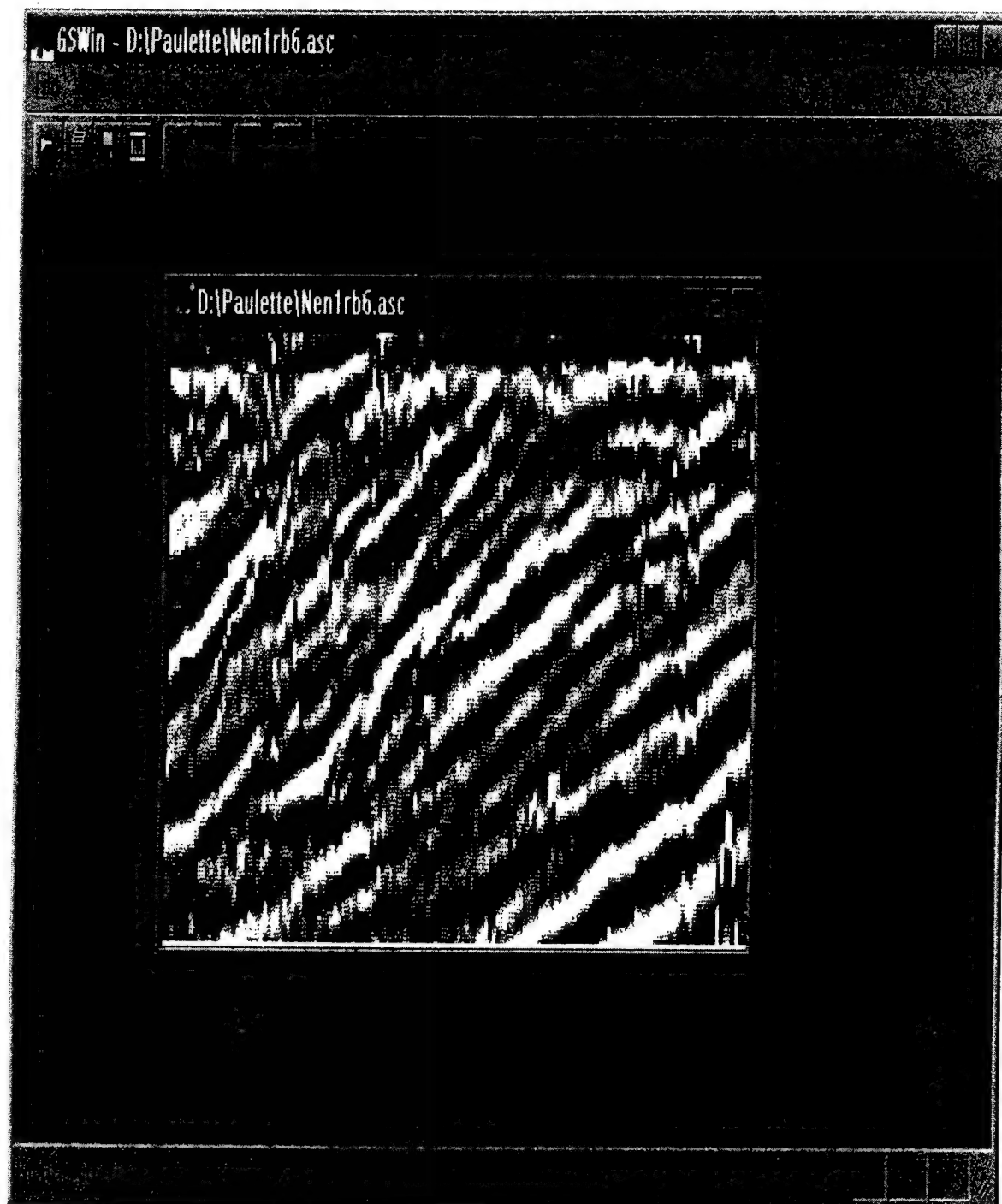


**Figure 2.1.** Data imported from PULSE EKKO format.

is done by comparing all points in the grid to each other. The user can choose to select a rectangular or irregular region on which to perform the analysis if the entire data set is not desired. In this way it is possible to separate for analysis regions in the GPR image that represent different geologic units. These options appear in the toolbar as well the pull-down menus. Once the mode is set, the user draws the region by holding the left mouse button and moving the mouse. When a region has been selected, clicking the semivariogram toolbar button ( $\gamma$ ) gives the user a list of options (Figure 2.2) for computing the variogram surface. The user can either change the number of lags, which determines the number of data points in the plot, the lag spacing, which indicates how many metres each pixel in the semivariogram represents, or leave them on the defaults. These defaults are the x and y sampling rates for the data set, and 30 pixels in each direction. Once these are specified the program computes a two-dimensional semivariogram on the data (Figure 2.3). This window is split in two, one containing the actual semivariogram, the other showing the number of pixels and lag spacing. In order to calculate the one dimensional semivariogram in a particular direction, which is the ultimate goal, the user clicks on a portion of the variogram surface with the left mouse button and a line is drawn from the center out to that point and the angle is calculated. This line can then be moved by moving the mouse and holding down the left button. When the angle is to the user's satisfaction, the 1-D semivariogram is calculated (Figure 2.4) when the user releases the left mouse button.

An experimental semivariogram results in values for  $\gamma$  only at certain lags, which are determined by the sampling interval of the data. Semivariogram models are used to provide an analytic description of the experimental semivariogram so that  $\gamma$  can be calculated for any lag  $h$ . This is needed in order to use the semivariogram for simulation algorithms and to provide a better estimate of the true correlation length of the data set. In Figure 2.4 the 1-D semivariogram window is a split window showing the semivariogram in the left half and the fitting parameters in the right.



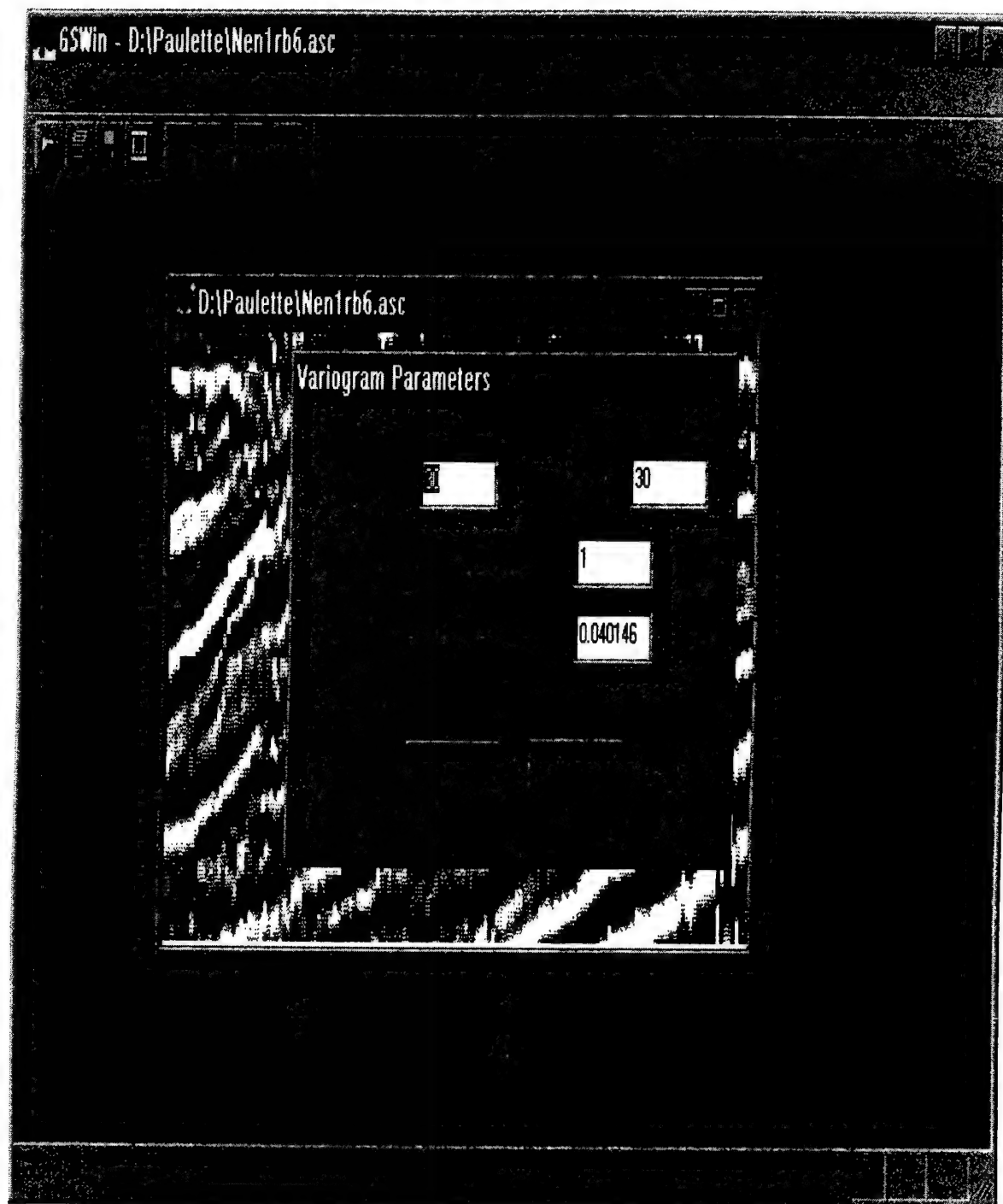


**Figure 2.2.** The options for the variogram computation.

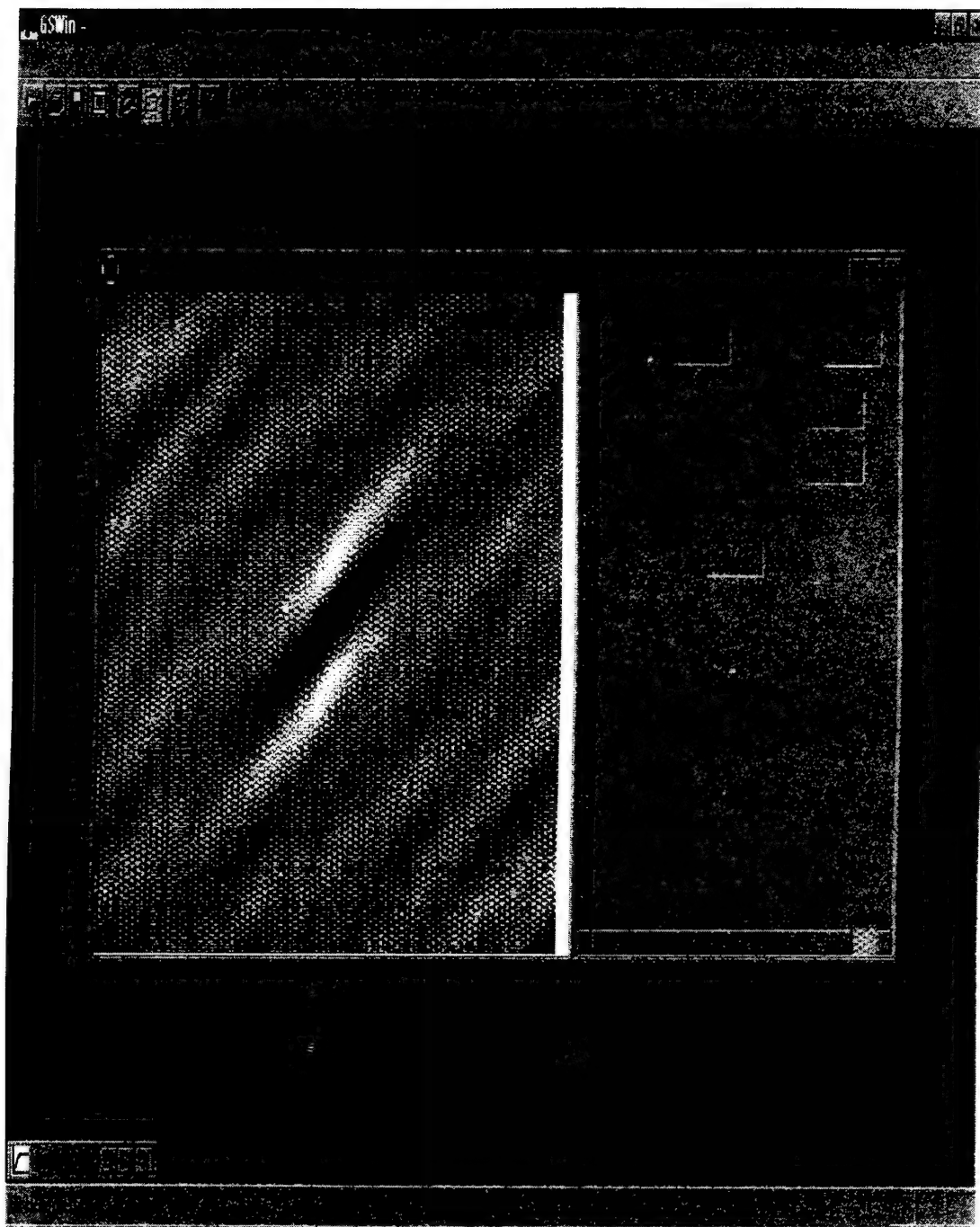


**Figure 2.3.** Two dimensional variogram. The angle of the dark ellipse indicates the maximum correlation direction.

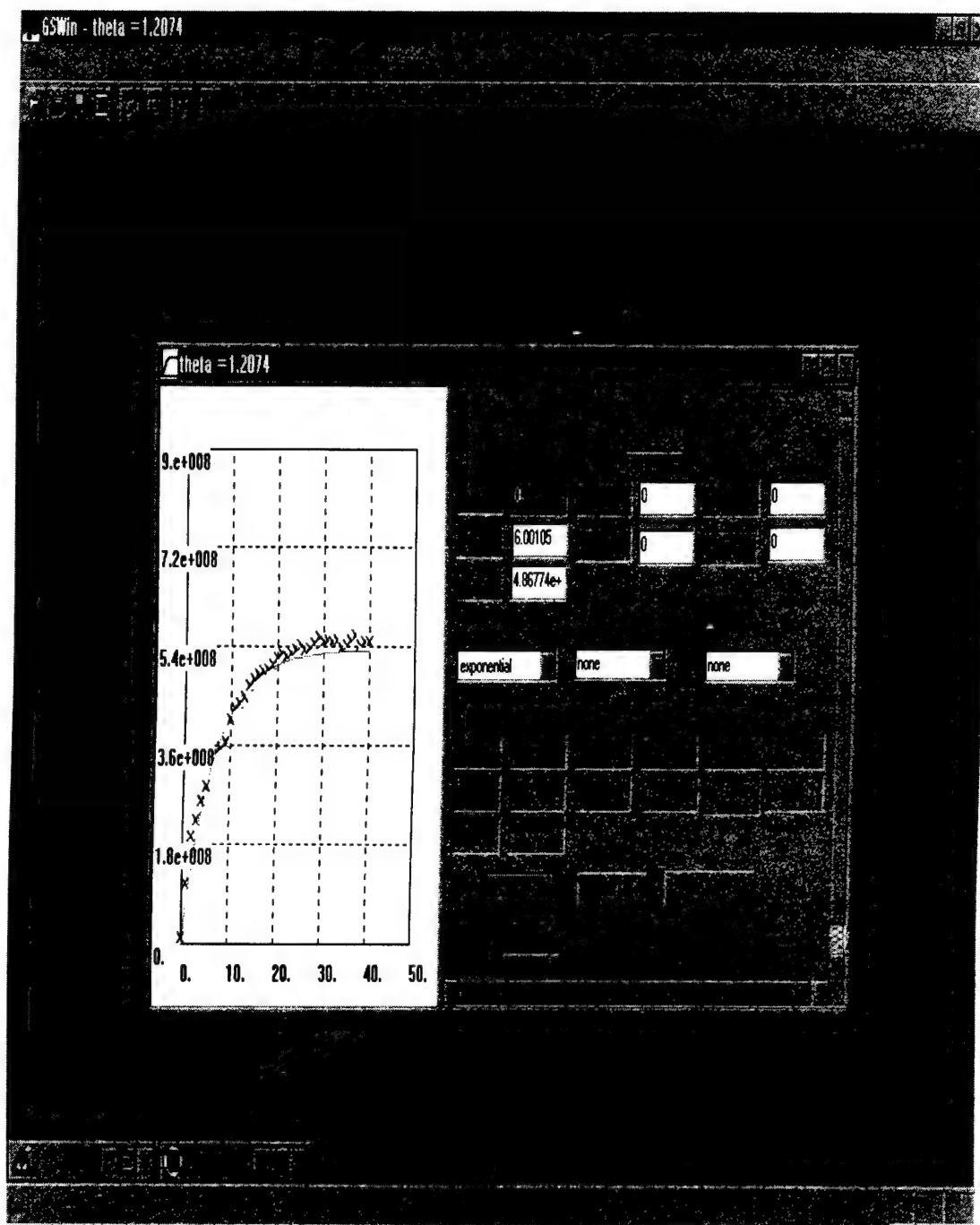


Figure 2.4. A one dimensional variogram. The exponential model was the best fit in this case.

Here the user can determine which model best fits the data. The models which the program supports are as follows (Jian et al, 1996):

### 1.Spherical

$$\gamma(h) = \begin{cases} C_0(1-H(h)) + C\left(\frac{3h}{2a} - \frac{1}{2}\left(\frac{h}{a}\right)^3\right), & 0 \leq h < a \\ C_0 + C, & a \leq h \end{cases}$$

### 2.Exponential

$$\gamma(h) = C_0(1-H(h)) + C\left(1 - e^{-\frac{3h}{a}}\right), \quad 0 \leq h$$

### 3.Power

$$\gamma(h) = C_0(1-H(h)) + \alpha h^\beta, \quad 0 < \beta < 2; \quad 0 \leq h$$

### 4.Gaussian

$$\gamma(h) = C_0(1-H(h)) + C\left(1 - e^{-3\left(\frac{h}{a}\right)^2}\right), \quad 0 \leq h$$

### 5.Cubic

$$\gamma(h) = \begin{cases} C_0(1-H(h)) + C\left(7\left(\frac{h}{a}\right)^2 - \frac{35}{4}\left(\frac{h}{a}\right)^3 + \frac{7}{2}\left(\frac{h}{a}\right)^5 - \frac{3}{4}\left(\frac{h}{a}\right)^7\right), & 0 \leq h < a \\ C_0 + C, & a \leq h \end{cases}$$

### 6. Pentaspherical

$$\gamma(h) = \begin{cases} C_0(1 - H(h)) + C \left( \frac{15h}{8a} - \frac{5}{4} \left( \frac{h}{a} \right)^3 + \frac{3}{8} \left( \frac{h}{a} \right)^5 \right), & 0 \leq h < a \\ C_0 + C, & a \leq h \end{cases}$$

### 7. Hole Effect

$$\gamma(h) = C_0(1 - H(h)) + C \left( 1 - \frac{\sin \left( 4.4934 \frac{h}{a} \right)}{4.4934 \frac{h}{a}} \right), \quad 0 \leq h$$

where

$$H(h) = \begin{cases} 0 & h > 0 \\ 1 & h = 0 \end{cases}$$

$C_0$  = nugget

$a$  = range

$C$  = sill

In order to determine the best-fit model, the user can press the 'best fit' button shown in Figure 2.4 and the program will perform a nonlinear least-squares fit using each model. The one with the lowest resulting  $\chi^2$  is chosen as the best-fit. The fitted semivariogram is drawn in the left window using a green line. A nested model (linear combination) of up to three different models may also be used by specifying the models in the boxes and choosing 'fit'. The initial guesses, which appear in the top half of the window, can be changed by the user, though the defaults are often

close to the final value anyway. The defaults are chosen by an algorithm which guesses at the range by estimating where the graph begins to level out. The sill is chosen by averaging all points after this estimated range. The user can also select an individual model and press the 'fit' button to determine the parameters for a particular model. Once the analysis is complete, the user can choose to save the semivariogram along with all the fitted parameters so it may be loaded into a graphing package, such as Excel. The user can also reduce the number of points to be fit by clicking the left mouse button on the variogram window and moving the cutoff line to the desired position.

This program was written using Microsoft Visual C++. The nonlinear least squares fitting routine uses the Levenberg-Marquardt technique as implemented in Numerical Recipes (Press et al, 1992). The calculation of the 2-D semivariogram was based on a routine from GSLIB which was converted to C++ from its original FORTRAN.

### **Calibration Field Experiment**

Our working hypothesis is that the correlation structure determined for the GPR image is a valid description of the correlation structure of the hydraulic properties of the subsurface. This assumes that the spatial variation in dielectric properties, seen in the GPR data, is an accurate image of the spatial variation in hydraulic properties of the subsurface. The critical issue which must be addressed then is the relationship between the GPR image and the properties of the subsurface. Determining this link, between the GPR image and the "geological reality" is a key part of our research. The approach that we are taking is to conduct cliff face studies: GPR data are collected along the top of the cliff and the imaged section can be seen and sampled. This offers an outstanding opportunity to determine what is really imaged in the GPR section; i.e. to "ground truth" the GPR data.

In one cliff face experiment (described in Rea and Knight, 1998) we compared the geostatistical analysis of a photographic image and a GPR image of a sequence of alternating coarse sand, and fine sand and silt. The digital photograph of the face captured information about the spatial distribution of coarse grained and fine grained beds on the basis of gray scale. There was excellent agreement between the variograms from the photograph and the radar data, in determining both the maximum correlation direction and the correlation length. These results led us to conclude that the GPR data did in fact image the spatial distribution of these two lithologies and could be used to quantify both the correlation direction and length in this sedimentary unit. In this example the spatial variation in dielectric properties in the subsurface was closely related to the spatial variation in grain size; this is very reasonable given what is known about the relationship between dielectric properties and sedimentary properties.

### **Analysis of GPR Data from Selected Depositional Environments**

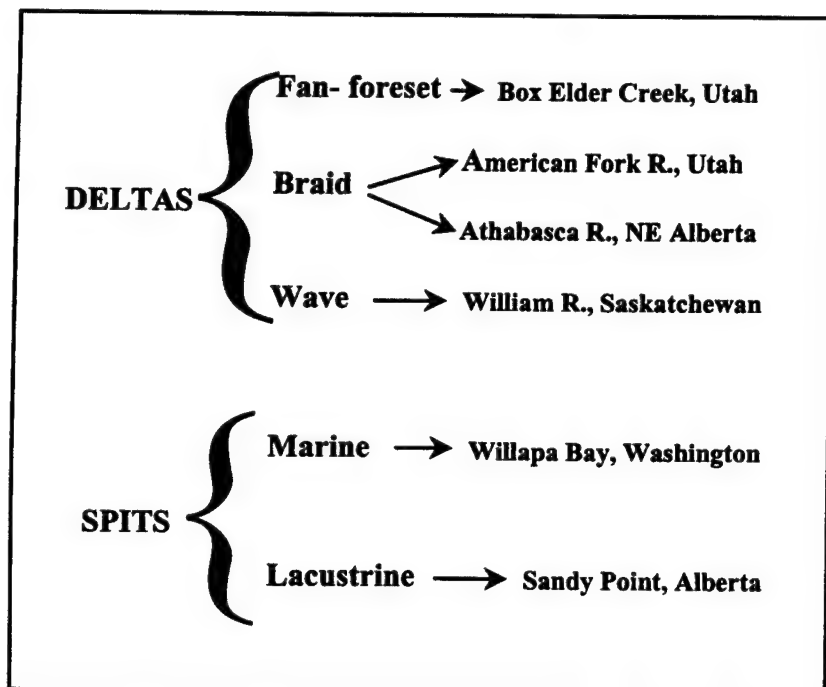
In collaboration with Harry Jol, University of Wisconsin Eau-Claire, we conducted geostatistical analyses of GPR images from a variety of selected depositional environments. We had two principal objectives in this work. The first was to determine whether the geostatistical analysis of GPR data, that we had shown to be successful in the cliff-face example described in Rea and Knight (1998), would be successful in a wide range of sedimentary environments. Our second objective was to investigate a more fundamental issue: We suggest that the physical and chemical processes acting in any given depositional environment should be responsible for determining the spatial heterogeneity in material (e.g. hydraulic) properties in that environment. We want to test the idea that this will lead to different depositional environments having different but "characteristic" geostatistical signatures. That is, the semivariograms that represent sedimentary packages from braided streams will all have certain features in common, and will differ in predictable ways from semivariograms for sedimentary packages from coastal spits. The



characteristic features might be the correlation length or the functional form of the semivariogram (exponential, spherical, nested etc.).

The depositional environments that we have examined are listed in Table 2.1. In our work we have achieved our first objective - the geostatistical analysis of GPR data can be conducted in a wide range of depositional environments. In all cases we have obtained outstanding experimental semivariograms that are well-modeled by the standard semivariograms models. With respect to our second objective, we do observe differences in the geostatistical "signature" of different environments, and can make some general conclusions about the relationship between depositional processes and the resulting spatial statistics. However, further work is required to develop a more fundamental understanding of the link between depositional environments and their geostatistical character. The preliminary results from this work are described in detail in Knight et al. (1997); the final results were presented recently at the Hazardous Substances Research Conference (Knight et al., 1998) and are in preparation as a paper to be submitted to the journal *Geophysics*. Our principal findings are briefly described below.

Table 2.2 lists the results of the geostatistical analysis of the GPR images. We find correlation lengths ranging from 3m to 53 m and find that an exponential model best describes the majority of the data. As one example of the differences we see in the geostatistical signature of different environments, we can compare the GPR image of a fan-foreset delta and the GPR image of a braid delta. As can be seen in the GPR image of the fan-foreset delta (Figure 2.5) this environment contains long continuous dipping features that are found to have a maximum correlation direction of 20° to the northwest.. These features in the GPR data are interpreted to represent the foreset beds within the delta. In Figure 2.6 is shown the experimental semivariogram in that direction, with a correlation length of 53 m. In contrast to the depositional environment for a fan-foreset delta, which tends to produce and preserve long, continuous bedding planes, a braid delta is formed in an environment dominated by high fluctuations in energy level. As can be seen in the

**Table 2.1. Depositional Environment**

**Table 2.2. Semivariogram analysis: parameters and results**

Environment & Location			Facies	Angle (°)	model	range (m)
DELTA	FAN - FORESET	Box Elder Creek	Foreset	20 NW	exp. gauss.	53 3
	BRAID	American Forks R.	Cut and Fill	0.5	exp.	3
		Athabasca River	A (cut and fill)	1 W-NW	exp.	6
			B (cut and fill)	1 E-SE	exp.	4
			C (cut and fill)	1 E-SE	exp.	5
		William River	D (cut and fill)	0	exp.	4
	WAVE	William River	Uppershore/ Beachface	1E	exp.	7
			Lower-mid shore	2E	pent.	14
SPITS	MARINE	Willapa Bay	Dip Beachface	1.5 W	exp.	24
			Strike Beachface	0	sph. gauss.	6 46
	LACUSTRINE	Sandy Point	Beachface	1 SE	pent.	18
			Beachface ⊥	0	sph.	7
			Stormzone	2 SE	exp.	7
			Stormzone ⊥	3 SW	exp.	10
			Lakebed	0	exp.	43
			Lakebed ⊥	2 SW	exp.	9

exp. = exponential, gauss. = gaussian, pent. = pentaspherical, sph. = spherical

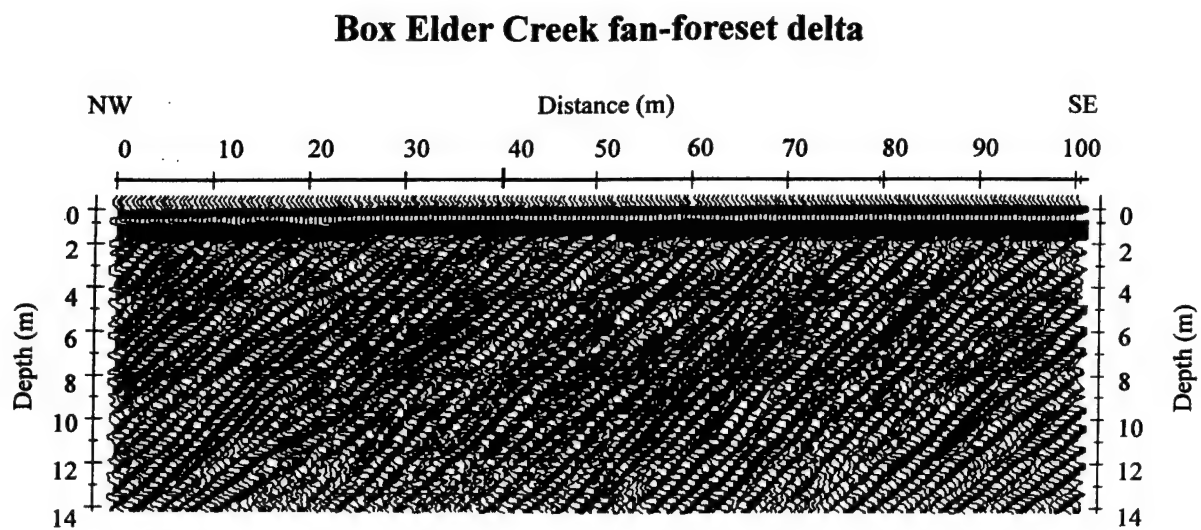


**Figure 2.5.** GPR profile collected over the fan-foreset delta (modified from Smith and Jol, 1992a).

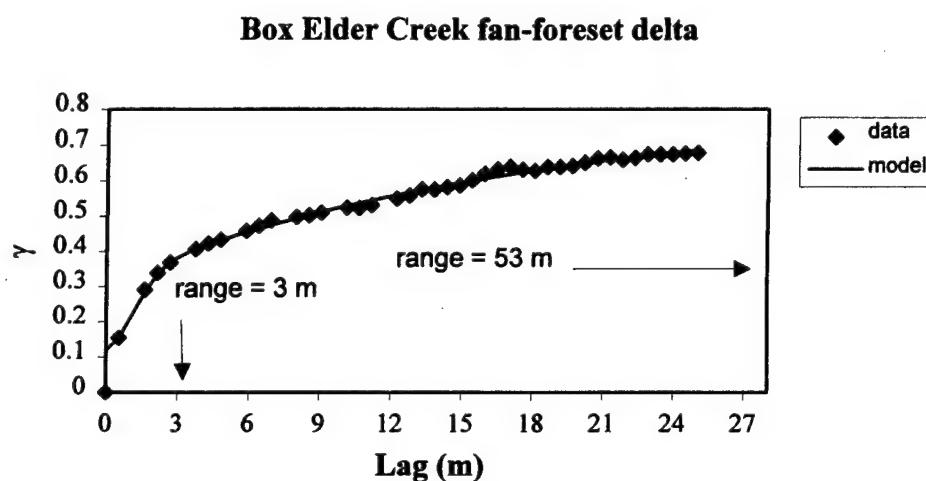


**Figure 2.6** Semivariogram of the GPR data collected over the Box Elder Creek delta foreset beds shown in Figure 2.5. The data points are the circles; the model of the semivariogram is the solid line. These data are modeled using a nested exponential and gaussian model with ranges of 53 m and 3 m. This very long range, 53 m, is a measure of the distance over which the inclined strata are continuous.

GPR image from a braid delta (Figure 2.7), the section is made up of numerous discontinuous features that are interpreted as "cut and fill" structures which reflect the continuous shifting of the channel position. The semivariogram from this environment, shown in Figure 2.8, has a correlation length of 3m. Clearly we see in the geostatistical "signature" of these two deltas what we would expect given the nature of the depositional environments - long correlation lengths in the fan-foreset delta, and much shorter correlation lengths in the braid delta.

As a second example of differences in correlation structure due to differences in depositional processes we show in Figure 2.9 the GPR data from a lacustrine spit. In this case there is a change in depositional processes with time - which corresponds to progradation of the spit into the lake. In analyzing this data set GSWIN proved to be extremely useful, as we could select and analyze separately three regions in the data, as shown on the GPR section. Again, in this example we see differences in the semivariograms (Figures 2.10 a,b,c) that can be qualitatively related to the depositional processes. The lake bed represented by long, horizontal reflections has a maximum correlation length of 43m. The storm generated deposits reflect a high energy environment and are characterized by shorter, dipping reflectors with a correlation of 7m. The beach face which corresponds to the zone of wave swash is represented by long horizontal reflections with a correlation length of 18m.

As can be seen in the above examples, the quality of the all the variograms are outstanding. We conclude that geostatistical analysis of GPR data can be applied in a variety of geological environments. The examples also illustrate the concept which we have begun to investigate - can the variograms from different environment be explained in terms of the processes occurring in the environments?; and is there a characteristic geostatistical "signature" associated with specific environments? Such signatures would be extremely useful in attempting to interpret and integrate data at a site if there was some prior knowledge of the depositional environment.

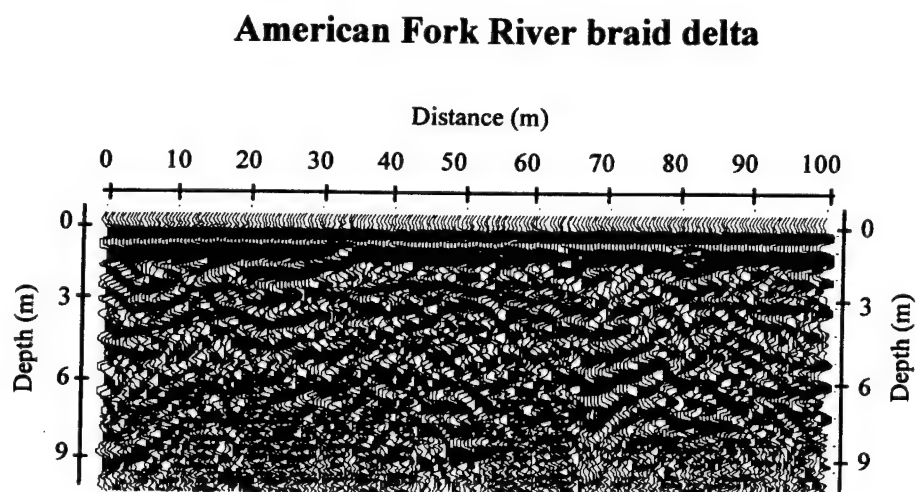


**Figure 2.7.** GPR profile collected over the American Fork River braid delta (modified from Jol and Smith, 1992).



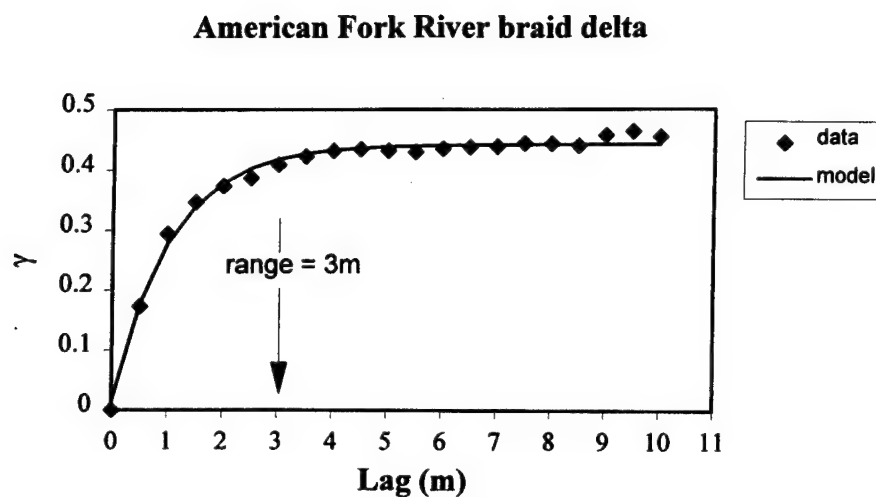


**Figure 2.8.** Semivariogram analysis of the GPR image shown in Figure 2.7. The data points are the circles; the model of the semivariogram is the solid line. These data are modeled using an exponential model with a range of 3 m. These short discontinuous reflectors have been interpreted as cut and fill structures.

### Sandy Point spit: parallel to spit axis

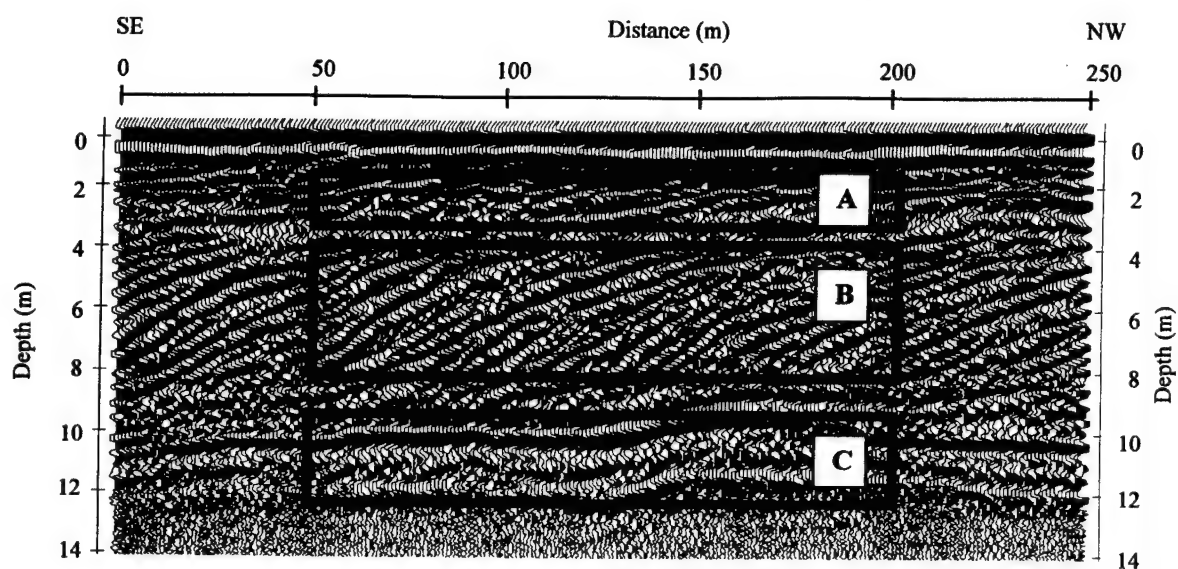


**Figure 2.9.** GPR profile collected parallel to the spit axis over the active Sandy Point spit (modified from Smith and Jol, 1992b). Areas outlined indicate data used in geostatistical analysis. Area "A" represents beachface/upper shoreface, area "B" represents storm influenced zone, and area "C" represents the lake bed.

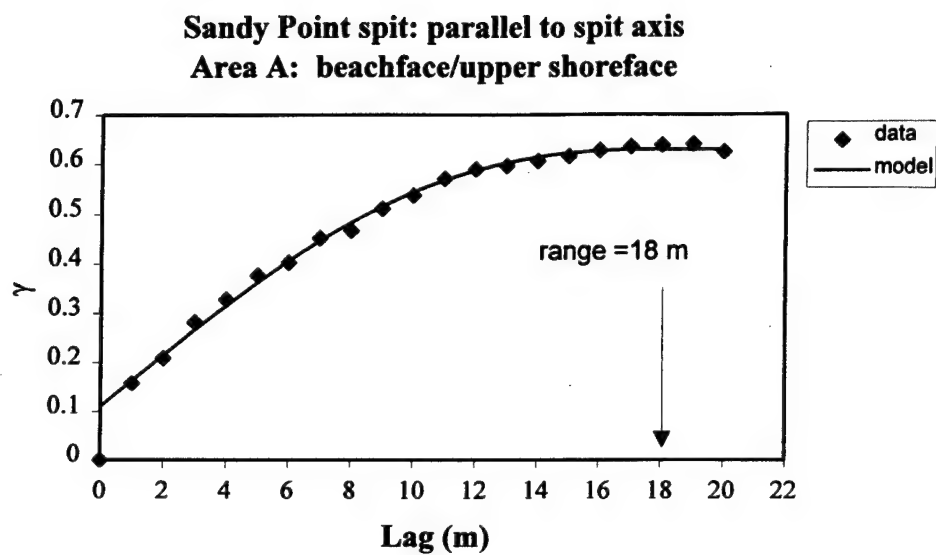


**Figure 2.10a.** Semivariogram analysis of area “A” in Figure 2.9. These data are modeled using a pentaspherical model with a range of 18 m.

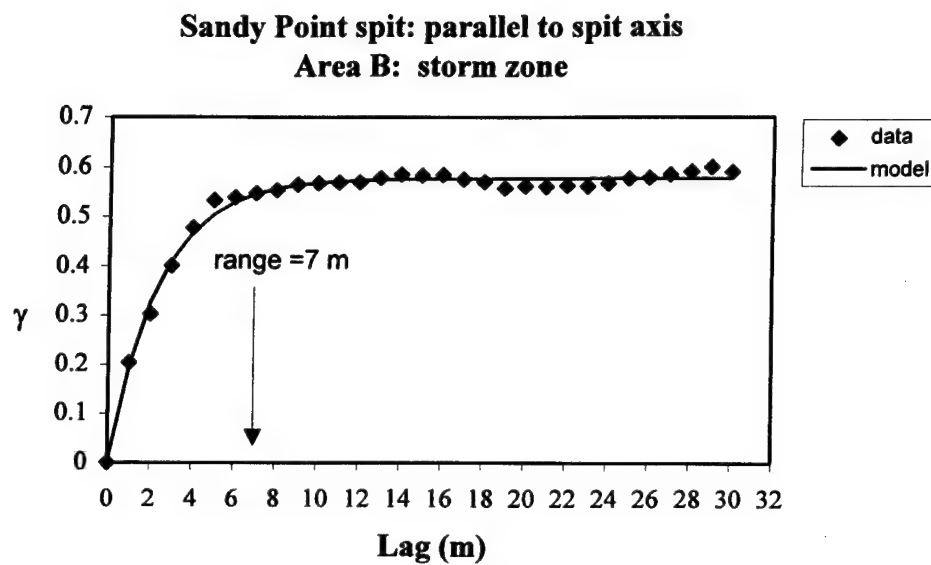


**Figure 2.10b.** Semivariogram analysis of area “B” in Figure 2.9. These data are modeled using an exponential model with a range of 7 m.

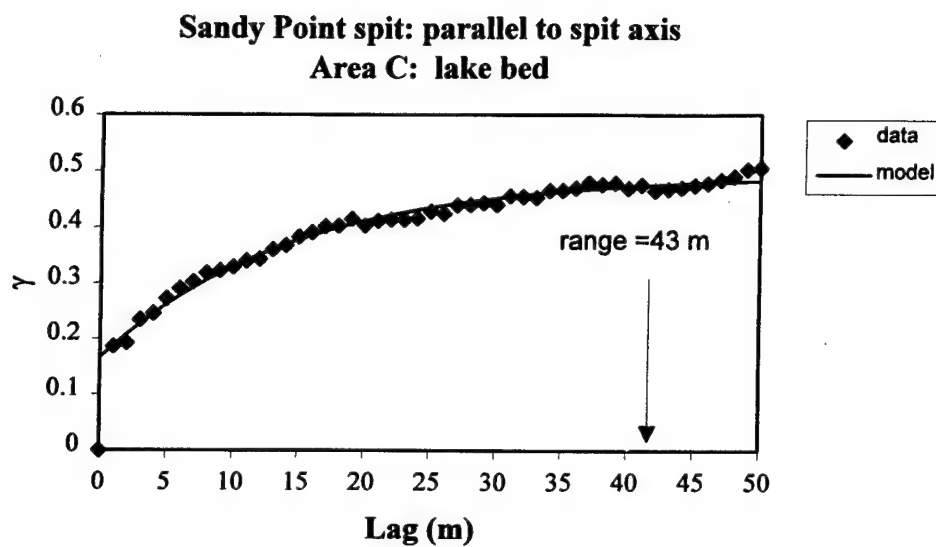


**Figure 2.10c.** Semivariogram analysis of area “C” in Figure 2.9. These data are modeled using an exponential model with a range of 43 m.

## Conclusions

The results presented in this section illustrate the potential value of using GPR images of the subsurface to describe and quantify the nature of the spatial heterogeneity in the subsurface. Such information could be used at the start of a site characterization exercise in order to plan the spacing and density required for drilling and direct sampling. In addition, the correlation structure imaged with GPR could be used to assist in the integration and interpretation of data from a site. Inevitably, in the assessment of any site there will be a shortage of data. Information about spatial variability, as can be provided by GPR images, can assist in developing models of the subsurface that adequately account for the heterogeneity in hydraulic properties.

## 3

## **The Relationship Between Dielectric Constant and Hydraulic Properties**

### **Introduction**

Of interest in our research is an assessment of the ways in which measurements of dielectric properties of the subsurface can be used to obtain information about hydrogeologic properties. In the previous section we described a methodology for using GPR images (i.e. dielectric images) to characterize the spatial heterogeneity in subsurface materials. In this chapter we describe research focused on using measurements of the dielectric constant of a volume of the subsurface to obtain estimates of the magnitude of hydrogeologic properties. That is, can we measure the dielectric constant of an area and from that obtain accurate estimates of water content, porosity, permeability?

There are two methods commonly used to determine the dielectric constant of a region in the subsurface. In time domain reflectometry (TDR) the dielectric constant is calculated from the time it takes an electromagnetic (EM) wave to travel along the TDR probe, a wave guide, inserted into the ground. The sampled material over which the dielectric constant is determined is the volume of material immediately adjacent to and along the full length of the TDR probe. A TDR study is most commonly conducted to assess the variation in water content in the top few meters of the earth and typically covers an area of tens of square meters with sample spacing on the order of a meter.

Dielectric information can also be obtained using a ground penetrating radar (GPR) system. In using GPR, two antennae are moved across the earth's surface: one to transmit electromagnetic energy and the other to receive energy that has been reflected back to the surface from interfaces across which there have been changes in dielectric properties. The volume of the subsurface

sampled in GPR studies usually ranges from hundreds to thousands of cubic meters. The dielectric constant of a region determines the velocity of the electromagnetic wave such that GPR velocity data can be used to obtain a model of the dielectric constant of the subsurface.

The relationship between the measured dielectric constant and the hydrogeologic properties (water saturation, porosity, permeability or hydraulic conductivity) is the key to our ability to transform measured values of dielectric constant in the subsurface to the hydrogeological properties of interest. Our concern is that all laboratory-derived relationships to date are for homogeneous samples. Similarly, all the theoretical and empirical relationships commonly used to relate dielectric measurements to other properties assume a homogeneous material. The unique aspect of our study is an assessment of the way in which the presence of heterogeneity changes the relationship between dielectric and hydrogeologic properties.

While we plan eventually to assess the relationships between dielectric constant and various hydrogeologic properties, we selected for this study the dielectric constant - water content relationship, as measurements of dielectric constant are most commonly conducted to monitor or estimate water content. In addition, we elected to start with a specific form of heterogeneity - layering. This is a form of heterogeneity commonly encountered as most TDR measurements and many GPR measurements are made in sedimentary environments where the soils, sediments, and rocks are complex interlayering of different lithologies. These layers commonly parallel the surface of the earth and can range in thickness from millimeters to many meters.

We divided this study into three parts - described in the three sections below. First the theoretical differences between the dielectric constant-water content and dielectric constant-water saturation relationships for homogeneous systems and layered systems were explored. We then numerically modeled the propagation of electromagnetic waves through layers of contrasting dielectric constants. Finally, laboratory measurements were made of electromagnetic velocity through



layers. From these three aspects of our study we have developed an improved understanding of TDR and GPR measurements in layered materials and suggest how this can lead to improved accuracy in the use of dielectric data to estimate hydrogeologic parameters.

## **Theoretical Study of Properties of Layered Materials**

### **Introduction**

This theoretical study examined the relationships between dielectric constant and water content and water saturation in layered materials. Our main objective in this study was to determine the level of inaccuracy in estimates of water content or saturation when the sampled system is incorrectly assumed to be homogeneous. The assumption of homogeneity, when layering is present, can introduce significant error into the determined water content or saturation levels. A complete description of this study is contained in Chan and Knight (1998) recently submitted to Water Resources Research; the main results are summarized below.

### **Description of Models and Theories**

Three model systems composed of sand and clay, sand and silty clay, and sand and silt loam were considered. In each of these systems the composition of the solid phase and the water/air content were varied. We first describe each of these systems as a homogeneous mixture of components and then as a set of layers. For each case, for each system, we theoretically predict the relationship between dielectric constant and water content and dielectric constant and water saturation.

In theoretically modeling the homogeneous system, a specific form of binary mixtures, previously studied by Nur et al. (1991) and Knoll and Knight (1996) was modeled. Water and air were assumed to be distributed evenly such that the average or global water content or saturation of the

sand-fine mixture can be considered to be uniform throughout the system. The relationships used to relate dielectric constant to water content and water saturation were the TP (time propagation) model and the Topp equation. These two models, which are commonly used to interpret measured dielectric constants, assume a homogeneous mixture of air, water, and solid.

The layered systems which were theoretically modeled were composed of the sand and fine fraction used in the homogeneous mixtures but arranged in distinct layers. Each layer was composed of a single sediment type. The volume fraction of fines was varied from 0 to 1 and the global water content from 0 to the value obtained when the pore space of the entire system is filled with water. A critical issue in the layered model was the heterogeneity that will exist in the distribution of water in the system. Under natural conditions differences in water content exist between sand and fine layers which in turn translate into differences in water saturation for the layers. In order to look at the dependence of dielectric constant on global water content or saturation in a layered sand-fine system, the water content and saturation of the individual layers were determined using Clapp and Hornberger's (1978) capillary pressure-saturation relationship. The dielectric constant of the individual layers were predicted using either the TP model or the Topp equation. These values were then used in calculating the average dielectric constant and the global water content and water saturation for the entire system.

The orientation of the layering and the thickness of the layers were additional variables in the modeling. We consider an electromagnetic (EM) wave traveling through the layered material, both parallel to and perpendicular to the layering. We consider two end-member cases where the wavelength of the EM wave is much greater than, and much less than, the thickness of the layers. In the first case, the average dielectric properties are modeled using an effective medium theory; in the second case, ray theory is used.

## Data/Results and Discussion

Plots of all the theoretical modeling results are found in Chan and Knight (1998). Figure 3.1 shows an example of the comparison of results from the theoretical calculations: the sand-clay system is shown at a fine fraction of 0.5. Both the dielectric constant–water content relationship (upper plot) and the dielectric constant–water saturation relationship (lower plot) are considered. The relationships for homogeneous systems are theoretically predicted using both TP and Topp. For the layered systems, the dielectric constants of individual layers were calculated using the TP model. We then model three cases of layered systems:

- 1) wave propagation direction is perpendicular to the layering, and the layer thickness is much less than the wavelength; this is referred to as “perpendicular EMT”.
- 2) wave propagation direction is perpendicular to the layering, and the layer thickness is much greater than the wavelength; this is referred to as “perpendicular ray”.
- 3) wave propagation direction is parallel to the layering, and the layer thickness is much less than the wavelength; this is referred to as “parallel EMT”.

The main objective in this study was to gain some insight into the errors that can be introduced in the determination of water content or saturation if the presence of layering in the natural system is not taken into account. The dielectric constant–water content and dielectric–water saturation relationships predicted for layered systems are used as the baselines for comparisons. As an example, let us consider a system (50% fine fraction) with thin layering perpendicular to the wave propagation direction. In Figure 3.2 are shown the errors that would result if water content and saturation were determined from dielectric measurements, and the system was assumed to be homogeneous; i.e. the presence of layering was neglected. The errors for water content are shown in the upper plot, while the errors for water saturation are shown in the lower plot. The errors for all three soil systems (sand-clay, sand-silty clay, and sand-silt loam) are shown for use of both the

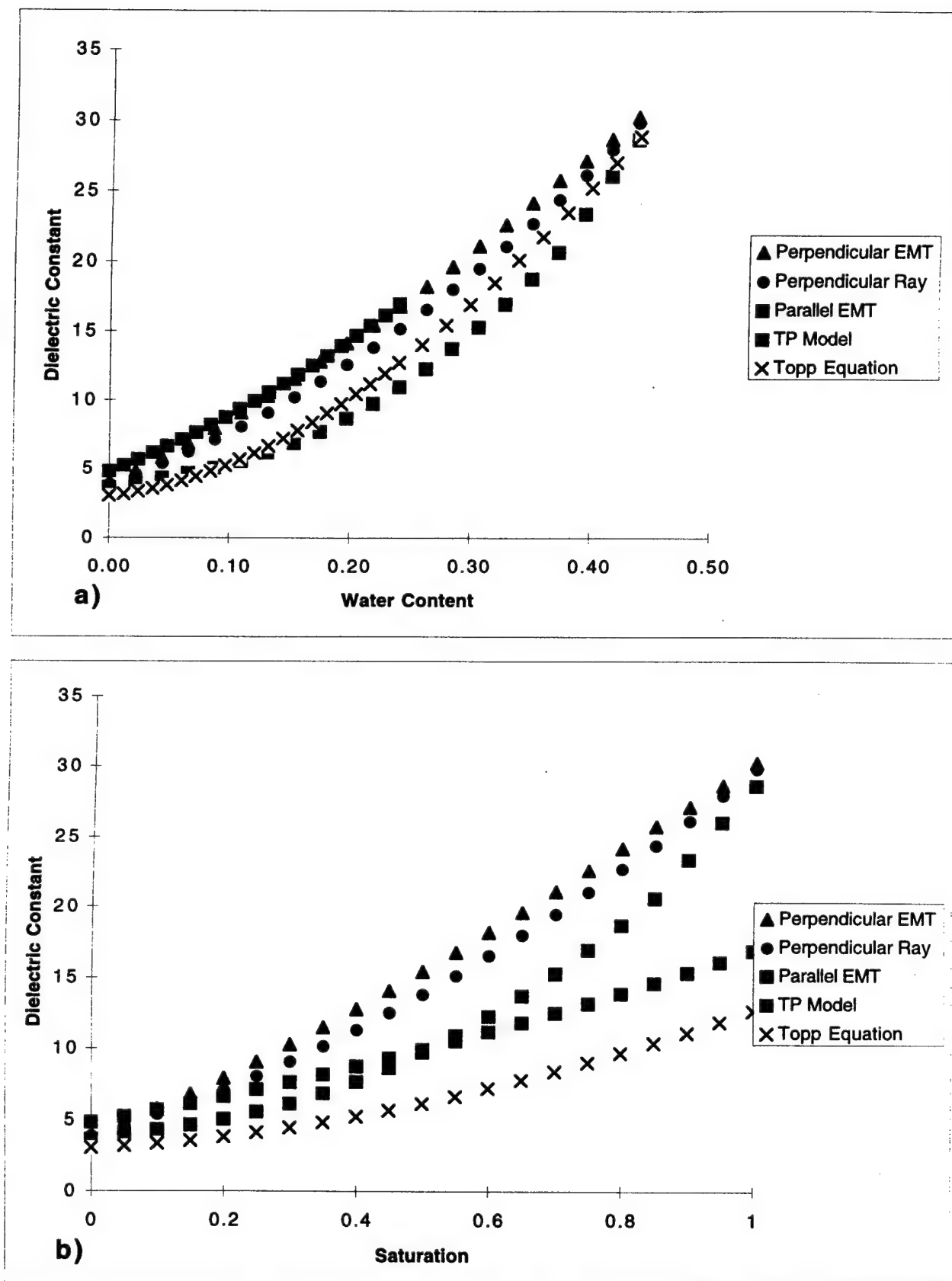


**Figure 3.1.** A comparison of dielectric constant calculated for the sand-clay system at a fine fraction of 0.50. a) Dielectric constant versus water content. b) Dielectric constant versus saturation.

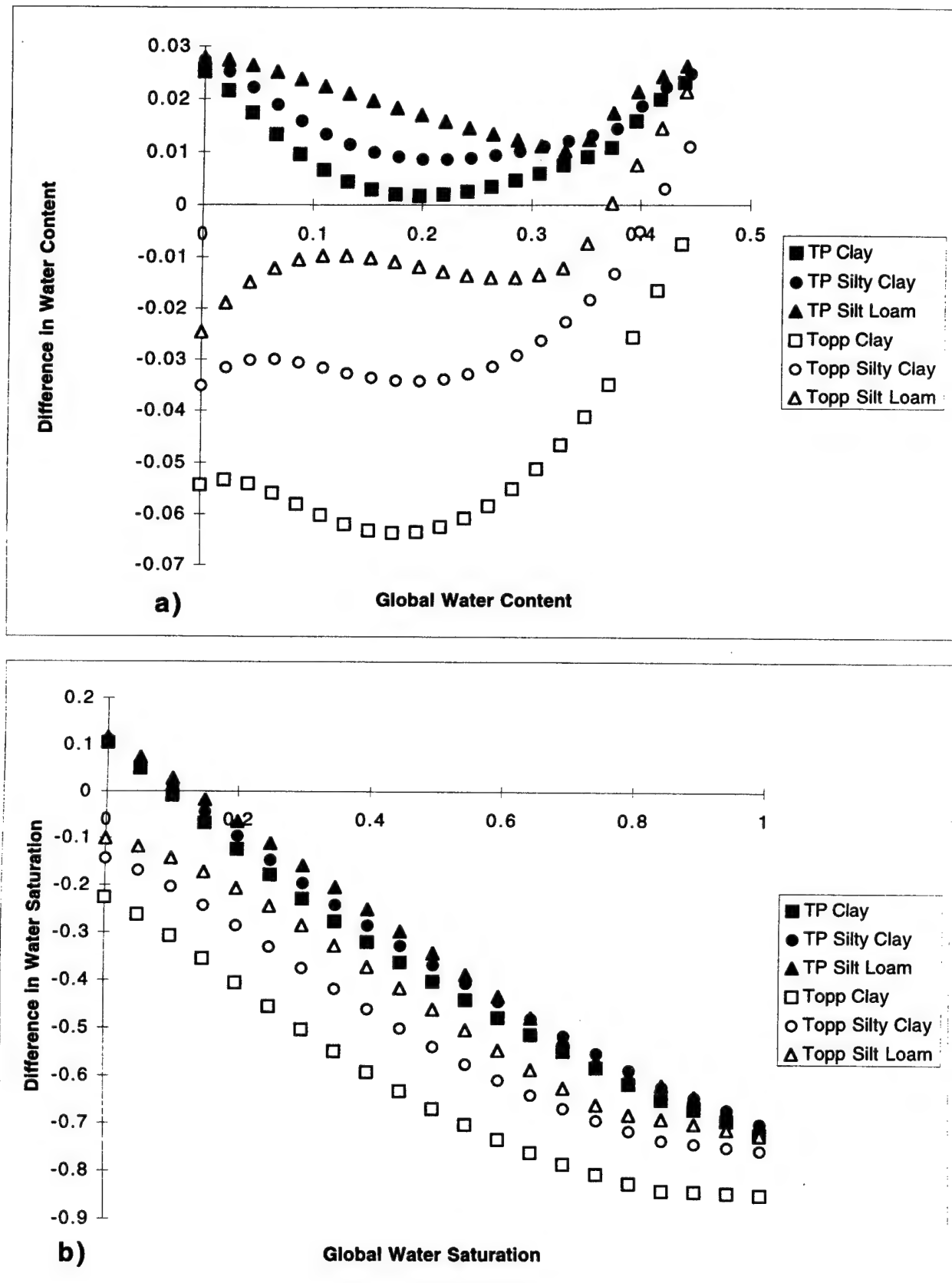


**Figure 3.2.** a) Difference between estimated and actual water content. b) Difference between estimated and actual water saturation. For EMT perpendicular to propagation for sand-fine systems at a 0.50 fine fraction.

TP model and the Topp equation. As can be seen in Figure 3.2, the errors in extracting water content can be as high as 0.064. The errors in extracting water saturation are even greater because of the effect of porosity due to the nature of the binary mixture for homogeneous systems.

## Conclusions

In summary, if sand-fine layers exist, using either the TP model or Topp equation to extract water content or saturation can produce significant errors. Often these errors fall outside the acceptable limits of  $\pm 0.03$  for water content and of  $\pm 0.05$  for water saturation. For all three layered scenarios, the TP model underestimates water content. In general, the Topp equation underestimates water content when thin layers exist parallel to the EM wave propagation but overestimates water content when either thin or thick layers are perpendicular to the propagation direction. However, the relationships for homogeneous systems tend to overestimate water saturation of layered systems. The errors become unacceptably large at higher water saturations and can even predict water saturations that have impossible values which are greater than 1.

## Numerical Modeling of EM Wave Propagation in Layered Systems

### Introduction

In Chan and Knight (1998), described briefly above, we model the relationship between dielectric constant and water content/saturation in homogeneous and layered systems of sand and fines. In the layered models, both the wavelength ( $\lambda$ ) of the EM wave and the average thickness ( $t$ ) of the layers are accounted for. When the wavelength is much larger than thickness of the layers,

effective medium theory (EMT) is used to calculate the average dielectric constant of the layers. When the wavelength is much smaller than the thickness of the layers, ray theory is used to calculate the average. The region over which each of these relationships is valid can be defined in terms of the ratio  $\lambda/t$ . It is this difference between the EMT and ray theory relationship that is the focus of this study: we wish to determine the exact region (defined by  $\lambda/t$ ) over which each relationship is valid. While it is clearly important to account for the presence of layering, it is also necessary to determine how the scale of the layering affects wave propagation, and the resulting sampled dielectric constant.

### Method of Numerical Analysis

The variable of interest in this study is  $\lambda/t$ , as this ratio defines the transition zone between a system which can be described using EMT and one which can be described using ray theory. The important parameter in finding the transition zone between EMT and ray theory is  $\lambda/t$ ; i.e. the ratio between the wavelength  $\lambda$  and the average thickness  $t$  of the layers.

Through numerical analysis the regimes for EMT and ray theory and the transition zone between them for EM waves were determined using a wave propagation matrix method written by Steven Cardimona. This program although based on wave propagation matrices uses the Kennett method for stability. The program calculates the travel time of an EM wave through a series of layers with given dielectric constants and conductivities. From the total travel time and the total thickness of layers, an average velocity can be calculated and compared to the velocities derived from the dielectric constants predicted from EMT and ray theory.

Wave propagation matrices are based on an exact solution to the 1-dimensional wave equation for a wave traveling through a series of layers. As described by Ward and Hohmann (1994), the electric and magnetic fields as seen in Figure 3.3 can be represented as a uniform plane wave:

$$E_{yi} = {}^+E_i e^{-ik_i(z-z_i)} + {}^-E_i e^{-ik_i(z-z_i)} \quad (1)$$

$$H_{xi} = -\frac{k_i}{\omega\mu_0} \left[ {}^+E_i e^{-ik_i(z-z_i)} + {}^-E_i e^{-ik_i(z-z_i)} \right] \quad (2)$$

where  $k_i$  is the complex wave number in the  $i^{\text{th}}$  layer,

$$k_i = \sqrt{\mu_i \epsilon_i \omega^2 - i\mu_i \sigma_i \omega} \quad (3)$$

$\omega$  is the angular frequency,  $\mu_0$  is the permeability of free space,  $\mu_i$  is the permeability of the  $i^{\text{th}}$  layer,  $\epsilon_i$  is the permittivity of the  $i^{\text{th}}$  layer,  $z_i$  is the vertical distance to the bottom of the  $i^{\text{th}}$  layer,  $z$  is any vertical distance within a layer at which the field is measured,  ${}^+E$  is the amplitude of the positive traveling electric wave in the  $i^{\text{th}}$  layer, and  ${}^-E$  is the amplitude of the negative traveling electric wave in the  $i^{\text{th}}$  layer.

Because both tangential EM fields must be continuous across layer boundaries, the EM fields immediately above a boundary can be rewritten in terms of the EM fields immediate below the boundary:

$$E_{y(i-1)} = {}^+E_{yi} \cosh(ik_i h_i) - Z_i H_{xi} \sinh(ik_i h_i) \quad (4)$$

$$H_{x(i-1)} = {}^+H_{xi} \cosh(ik_i h_i) - \frac{1}{Z_i} E_{yi} \sinh(ik_i h_i) \quad (5)$$



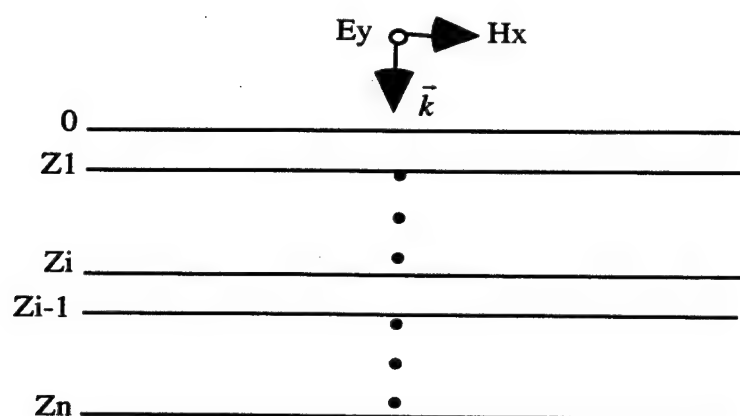


**Figure 3.3** A plane EM wave normally incident to a series of layers.  $E_y$ ,  $H_x$ , and  $\vec{k}$  are a right-handed orthogonal set.

where  $Z_i$  is the impedance of the  $i^{\text{th}}$  layer

$$Z_i = \frac{\omega\mu_0}{k_i} \quad (6)$$

and  $h_i$  is the thickness of the  $i^{\text{th}}$  layer. Since equations 4 and 5 are true at every boundary and since they can be written in matrix form, the EM fields at any given layer is simply the product of all the layers below it:

$$\begin{bmatrix} E_{y(i-1)} \\ H_{x(i-1)} \end{bmatrix} = \prod_{i=i}^n \begin{bmatrix} \cosh(ik_i h_i) & -Z_i \sinh(ik_i h_i) \\ -\frac{1}{Z_i} \sinh(ik_i h_i) & \cosh(ik_i h_i) \end{bmatrix} \begin{bmatrix} E_{y(n+1)} \\ H_{x(n+1)} \end{bmatrix} \quad (7)$$

These equations have been programmed to calculate the average dielectric constant of an EM wave through a set of layers. However, one must proscribe the boundary conditions at the lowest boundary; and in our case, we have set

$$H_{xn} = \frac{k_n}{\omega\mu_0} E_{xn} \quad (8)$$

so that there is no impedance contrast at this boundary and no reflection off the bottom back to the surface simulating a stack of layers over an infinite half-space with the same properties as the lowest layer. By changing both the thicknesses of the layers and/or the frequency of the wave, wave propagation in both the EMT and ray theory regimes can be simulated.

## Data/Results

Waveforms were numerically propagated at 50, 200, and 750 MHz through layered systems ranging from a wavelength to layer-set thickness ratio of less than 0.1 to greater than 10. The dielectric constants of the alternating equal layers were 15 and 5. In Figure 3.4 is an examples of the 50 MHz waveform modeled to arrive at the far end of the layered system. In all simulations we

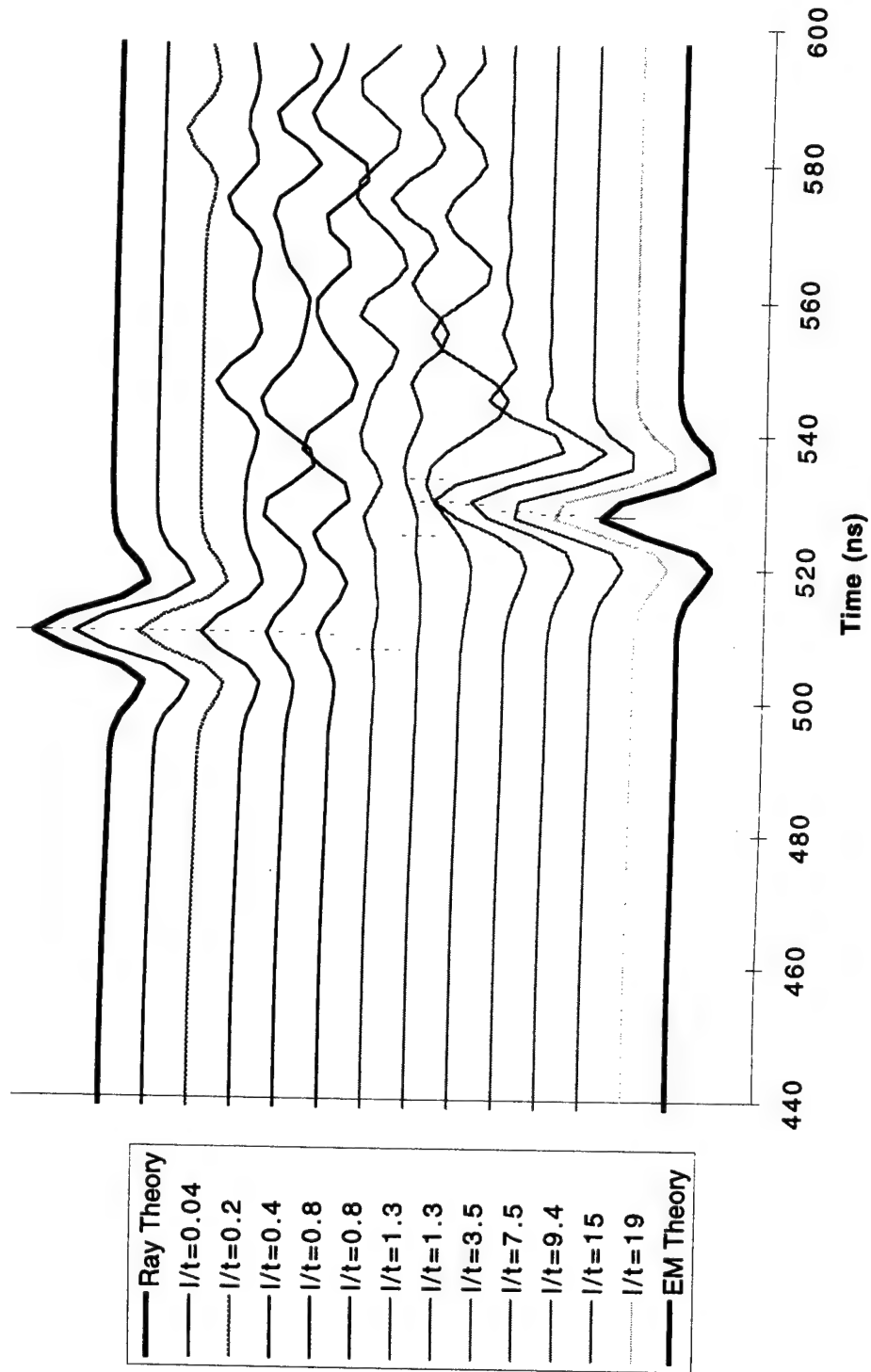


**Figure 3.4.** Waveforms at 50MHz. Half the layers have a dielectric constant of 15, and half have a dielectric constant of 5. The theoretical Ray theory and EM theory waveforms are shown in bold.

observe travel times increase as the layered section goes from a few thick layers (ray theory limit) to many thin layers (EMT limit). This is labeled on the plot in terms of the ratio of wavelength  $\lambda$  to layer thickness  $t$ . In the transition zone between the two limits, the waveforms become very attenuated due to scattering and the travel times are difficult to pick. Scattering also causes the wave to travel more slowly than theoretically expected.

In Figure 3.5, normalized EM velocity versus the wavelength to layer set thickness ratio is plotted for 50, 200, and 750 MHz. The ray theory and EMT limits are shown by the bold lines. Notice that the transition zone is quite narrow and is slightly higher than unity. Other calculations indicate that typical soil conductivities affect the amplitude of the waveforms but not the velocity of the wave. Also, the transition zone moves slightly to lower values when the proportion of high dielectric material is more than half and moves slightly closer to one when the proportion of high dielectric material is less than half. The transition zone is more distinct and farther from one when the contrast between the two materials is small but is more diffuse and slightly lower when the contrast between the two materials is large.

## Conclusions

The numerical wave propagation modeling confirms that the EMT relationship or the ray theory relationship for layered materials should be used for the interpretation of field data. Because the relationships for EMT and ray theory predict different dielectric constants for the proportions of sand and fines, one must determine which relationship should be used. The EMT relationship is valid when the wavelength to layer set thickness ratio is large while the ray theory relationship is valid when the ratio is small. In general, the transition zone between the two limits is narrow and occurs just below unity.

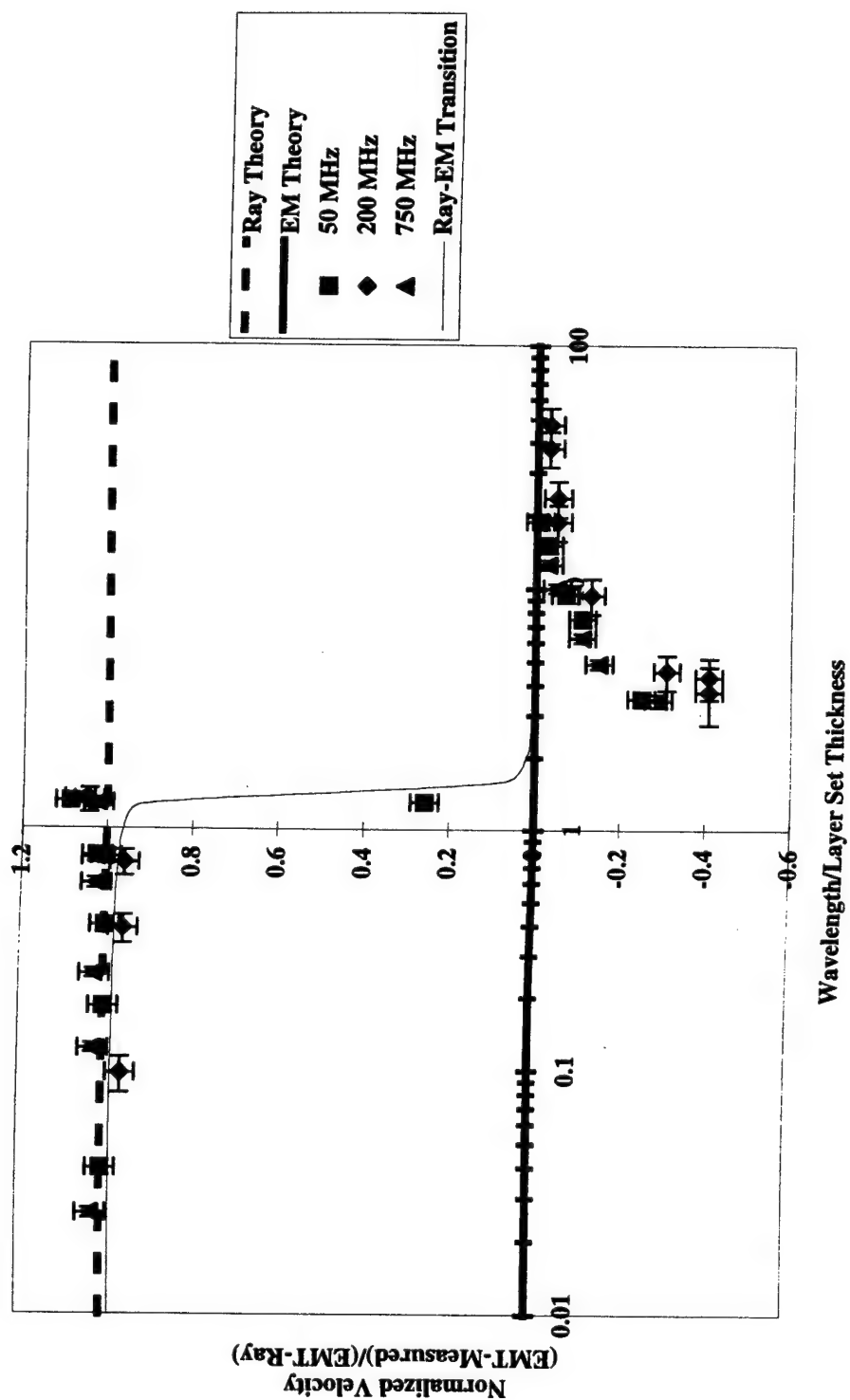


**Figure 3.5.** Normalized velocity versus wavelength to layer set thickness ratio from numerical study. Half the layers have a dielectric constant of 15, and half have a dielectric constant of 5.

## Laboratory Measurements

### Introduction/Experimental Methods

A series of laboratory experiments were conducted with systems composed of alternating layers of sand and silt. These experiments were designed to compare the theoretical and numerical predictions (described above) to results obtained through measurements on geological materials. We were interested in determining whether the transition from effective medium theory to ray theory could be observed experimentally.

The measurement apparatus consists of a center rod and a concentric outer shield. The center rod is 1 cm in diameter and the inner radius of the outer shield is 10 cm. Both the center rod and the outer shield are segmented into 10 cm pieces. The center rod segments screw together while the outer shield segments stack on top of each other. The outer shield segments are also scored every half centimeter and are sealed with O-rings. The total height of the apparatus is 1.20 m. However, because the apparatus is segmented, the total height does not need to be used for every measurement. The bottom segment is fixed to a base. In the base is a coaxial cable connection which connects the coaxial cell to the data collection instrument. Also in the base is a mechanical switch which causes a short between the center rod and the outer shield. The base also has a valve to allow fluid flow.

To pack the cylinder, a premeasured weight of soil is placed in the bottom segment of the cylinder and tamped down until it fills the desired layer thickness. For saturated layers, the calculated amount of water is poured onto a mesh which lies on top of the soil and distributes the water evenly throughout the soil. This process is repeated until the desired number of layers is reached. Cylinder segments are added to the apparatus as they are needed.

## Data Collection and Results

The data were collected using a Tektronix 1502C metallic cable tester TDR. This instrument is controlled by a 486 PC using an RS232 interface and the program TDR-Main written by David Redman at the University of Waterloo. This program records the amplitude of the TDR trace between two specified times. The data are converted to a text format and imported to MatLab for data analysis.

For each measurement three TDR traces are collected—an open trace, a trace where the cable is shorted at the base of the cylinder using the mechanical switch mentioned above, and a trace where the center rod and the outer sheath are shorted using a metal rod immediately above the top layer of soil. The three traces are plotted together. The times when the shorted traces deviate from the open trace are used to calculate the travel time through the sample and in turn the average dielectric constant.

In order to determine the accuracy of our apparatus, measurements were taken on air and water. Measurements were taken at every layer (ie every 10 cm) of the cylinder. The results are within a few percent of the expected values of approximately 1 and 80, respectively.

Data were collected on alternating layers of dry sand and saturated silt. Measurements were taken on layers 20 cm, 10 cm, and 1 cm in thickness. Assuming a frequency of 750 MHz, this corresponds to a ratio of wavelength to layer-set thickness ( $\lambda/t$ ) of approximately 0.3, 0.6, and 6.0, respectively. The dielectric constant of each layer was calculated using the TP model. The resulting values were then used to calculate the theoretical EMT and ray theory predictions. Figure 3.6 shows normalized EM wave velocity versus  $\lambda/t$ . This plot is very similar to Figure 3.5 and confirms that both EMT and ray theory limits are measurable. However, more data are needed to fill in the transition zone more fully.

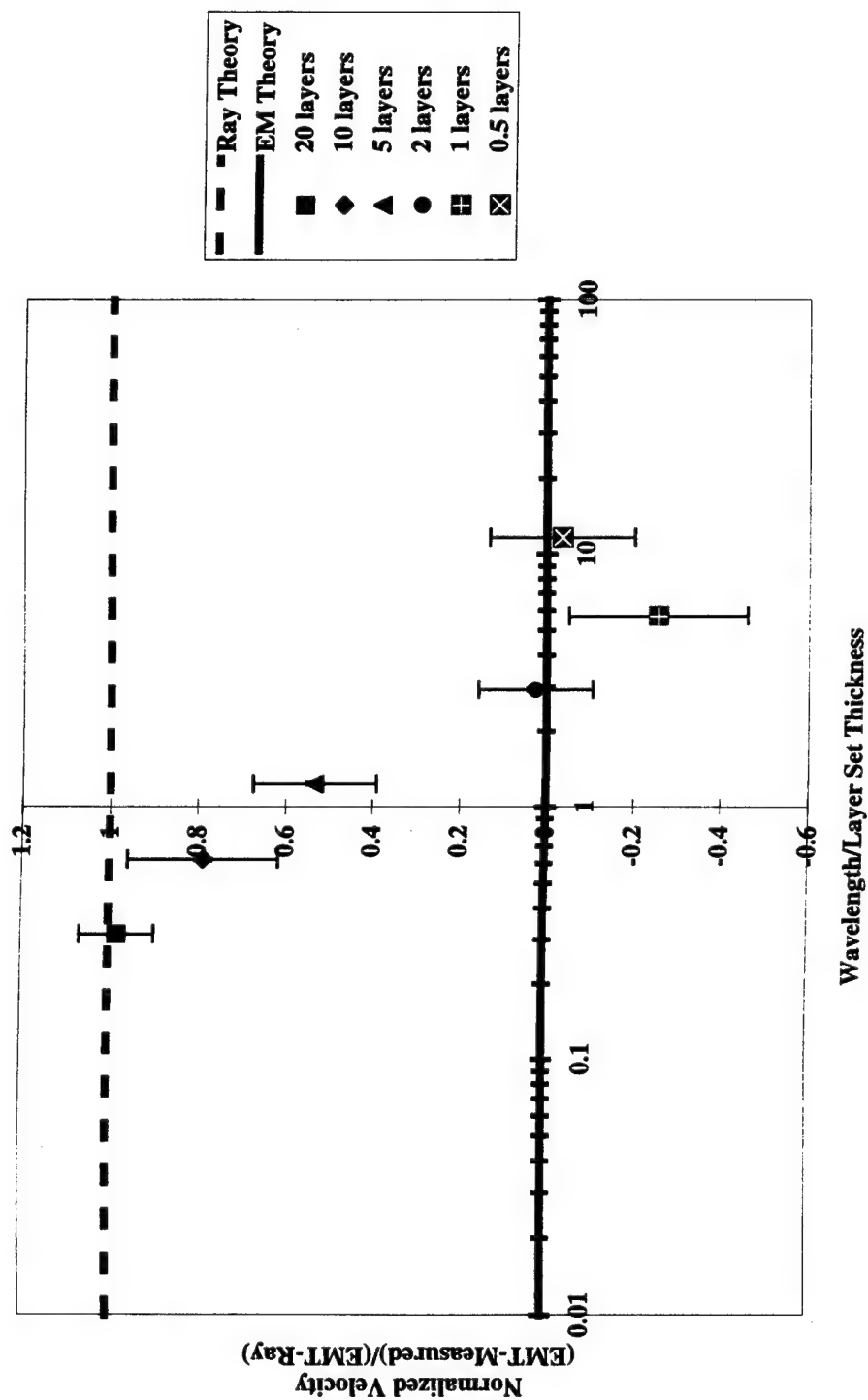


**Figure 3.6.** Normalized velocity versus wavelength to layer set thickness ratio from experimental study. Half the layers are wet silt, and half are dry sand.



## Conclusions

Laboratory data confirm that the EMT relationship or the ray theory relationship for layered materials should be used for the interpretation of dielectric constant. We observe a transition from EM velocities predicted by ray theory, at low values of  $\lambda/t$ , to EM velocities predicted by effective medium theory, at large values of  $\lambda/t$ . The transition zone between these two limits was found close to 1, as predicted by numerical modeling.

## CONCLUSIONS

Measurement of the dielectric constant of geological materials can be used to estimate hydraulic properties - but the accuracy of the determined hydraulic properties depends on the use of valid relationships to link dielectric properties to hydraulic. Most studies to date have been based on laboratory and theoretical results that use or assume homogeneous samples. In real materials there are likely to be layers of different materials present; these will affect both the measured dielectric constant and the relationship to hydraulic properties.

Our theoretical studies showed that significant error can be incurred if relationships for homogeneous systems such as the TP model or Topp equation are used to extract water content or saturation from the dielectric constant measurements of layered systems. Additionally, numerical EM wave propagation modeling showed that the wavelength to layer set thickness ratio of layered systems can also influence the average dielectric constant of a layered system. Finally, laboratory studies confirmed that both the EMT limit and the ray theory limit can be measured in sand and silt. The numerical and experimental results show a transition from ray theory to EMT at  $\lambda/t$  close to 1. We conclude that heterogeneity such as layering must be accounted for in order to accurately interpret dielectric measurements.

## 4

## Electrical Conductivity Estimates from GPR Data

A central theme in our research is the desire to use dielectric information, obtained from GPR data, to determine hydrogeologic properties. It is clear however that there is not a simple transform between these two types of properties. Additional information is required. The idea that we have investigated is that there exists in the GPR data itself additional information that is presently under-utilized. Specifically, GPR data contain information not only about dielectric properties, but also about electrical conductivity. This work is described in detail in the paper by Rea and Knight (1997), submitted to Geophysics.

The observed attenuation in GPR data contains information about the electrical conductivity of the subsurface. By quantifying all contributions to the attenuation recorded in the GPR data we can isolate and estimate the electrical conductivity. By far the most ill-constrained parameter in this method is the estimation of power loss associated with the partitioning of energy at interfaces - as some energy is transmitted and some is reflected at each interface across which there is a change in dielectric properties. We have concluded that the best approach is to attribute all loss due to energy splitting at interfaces to conductive loss; our analysis of the attenuation will then result in our obtaining a maximum or upper bound for the electrical conductivity.

We have found that this method can be used to quantify both lateral and vertical changes in electrical conductivity. We first tested the method at a site where there exists lateral variation in electrical conductivity (a sand and gravel unit adjacent to a clay-rich unit). At this location we had well control and conducted a DC resistivity survey along the same line. Conductivity measurements were also available from Time Domain Electromagnetic soundings at locations within 100 m of the line. The results that were obtained from our analysis of the 100 and 200 MHz GPR data are listed in Table 1 and compared with those from the DC resistivity and the

**Table 1** : Conductivity results from GPR decay rate analysis, and DC resistivity and TDEM surveys.

sedimentary unit	100 MHz GPR $\sigma$ (mS/m)	200 MHz GPR $\sigma$ (mS/m)	DC resistivity $\sigma$ (mS/m)	TDEM $\sigma$ (mS/m)
sand/gravel	3.5	4.3	0.2 - 1.6	0.1 - 5.0
clay	27	51	9.5 - 47	25-50

TDEM surveys. As can be seen, we obtained electrical conductivity estimates from the GPR data that are in very good agreement with those obtained from other methods.

At the second test site, a sand and gravel unit overlies a massive clay, producing a large vertical variation in electrical conductivity. We were able to see the response of each of these units and determined conductivity values that agreed well with other measurements at the site.

The attenuation seen in GPR data has long been interpreted in a qualitative way by practitioners in terms of conductivity; i.e. the observation of reduced signal penetration indicates a more conductive region. What we have shown in this study is that it is possible to extract a reasonable estimate of electrical conductivity from an analysis of the observed attenuation. This provides us with valuable complementary information and an additional parameter to help constrain the problem of obtaining a reliable model of the material or hydrogeologic properties of the subsurface from GPR data.

## 5

## Conclusions and Recommendations

The goal of our research is to develop an understanding of the link between dielectric properties and hydraulic properties of the subsurface. Measurements of dielectric properties of the subsurface can be obtained non-invasively from ground penetrating radar data. From an applied perspective our research can be described as addressing the question: How can we use these measurements of dielectric constant to characterize hydraulic conductivity at a site?

Our approach in this three-year research project has been a combination of field experiments, laboratory experiments, and theoretical modeling. Regardless of the approach, the emphasis has been to work with well-characterized materials, or field sites, so that we can study in detail the relationship between the hydrogeologic properties of geological materials and their dielectric properties.

There are two types of hydrogeologic information that have been the focus of our research. One type of information concerns obtaining estimates of the actual magnitude of hydrogeologic parameters; e.g. what is the porosity of this zone? what is the water content of the top meter? The other type of information concerns the spatial variability in hydrogeologic properties; e.g. over what distance do we expect to see continuity in permeable zones - meters or 10's of meters?

The first type of information can be obtained by taking measurements of dielectric properties of a volume of the subsurface and transforming it to obtain estimates of the hydraulic properties of that volume. The accuracy with which this can be done obviously depends heavily on the validity of the relationship that is used to transform dielectric measurements to hydraulic properties. Very commonly the assumption is made that the sampled volume is homogeneous; this being the underlying assumption in most relationships used to link dielectric and hydraulic properties. Our

theoretical, numerical and laboratory studies have addressed the effect of the presence of layering, and the importance of considering both the thickness of the layers  $t$  and the wavelength of the measurement  $\lambda$ . We find that when  $\lambda/t$  is less than 1 ray theory should be used is the interpretation of dielectric properties for hydraulic properties and when  $\lambda/t$  is great than 1, an effective medium theory should be used. We have calculated the error in involved in neglecting the effect of layering and find that it can be significant. The results from this aspect of our research suggest that heterogeneity should be considered in interpreting dielectric data; even if this only involves obtaining estimates of the likely errors involved in the interpretation of the data for hydrogeologic properties. In the natural world the assumption of heterogeneity is much more likely to be valid than the assumption of homogeneity.

The second type of required information involves describing the spatial heterogeneity of the subsurface. Often at a site there are some direct measurements of subsurface properties, but "filling in" between these measured data points requires knowledge of the structure or spatial variability of the subsurface, at that specific site. We have found that geostatistical analysis of GPR data can be used to characterize spatial variability in the subsurface, and have had tremendous success in analyzing data from a variety of depositional environments. This is an approach that we highly recommend being used at sites either in the initial planning stages, or to assist in the integration and interpretation of data. If it is possible to collect a GPR image at a site, that image is an excellent source of information about the heterogeneity of the subsurface. Further research in this area is needed to determine more specifically the link between the GPR image and the hydrogeologic properties - i.e. are we primarily imaging variation in water content, clay content, permeability, etc.? This is the critical question that must be answered in order to further the effective use of GPR for obtaining information about the nature and distribution of subsurface materials.

The combination of our field, laboratory and theoretical work has provided us with new ideas, and new approaches, to obtaining hydrogeologic information from dielectric measurements. In many applications in the earth sciences and engineering we are faced with the challenge of characterizing a complex, highly heterogeneous system. As we further our understanding of the link between dielectric properties and hydrogeological properties, we improve our ability to use dielectric measurements as a non-invasive means of characterizing the scale-dependent hydraulic properties of the subsurface.

## REFERENCES

- Chan, C. Y., and Knight, R. J., Determining water content and saturation from dielectric measurements of layered materials, submitted to Water Resources Research, 1998.
- Clapp, R. B., and G. M. Hornberger, Empirical equations for some soil hydraulic properties, *Water Resources Research*, 14, 601-604, 1978.
- Deutsch, C. V. and Journel, A. G., GSLIB Geostatistical Software Library and User's Guide, Oxford University Press, 1992.
- Jian, X., Olea, R.A., Yu, Yun-Sheng, "Semivariogram Modeling by Weighted Least Squares", *Computers and Geosciences*, 22, 387-397, 1996
- Jol, H. M. and Smith, D. G., Geometry and structure of deltas in large lakes: A ground penetrating radar overview, Geological Survey of Finland, Special Paper 16, 159-168, 1992.
- Knight, R., Tercier, P., and Jol, H., The role of ground penetrating radar and geostatistics in reservoir description, *The Leading Edge*, 1997.
- Knight, R., Tercier, P., Rea, J., Scullard, C., Jol, H., Geostatistical analysis of ground penetrating radar data, abstract, Hazardous Substance Research Conference, May 19-21, Snowbird Utah, 1998.
- Knoll, M. D., and R. J. Knight, Electrical properties of dry sand-clay mixtures in the frequency range 100 kHz to 10 MHz, *Geophysics*, submitted 1996.
- Nur, A., D. Marion, and H. Yin, Wave velocities in sediments, in *Shear waves in marine sediments*, edited by J. M. Hovem, M. D. Richardson and R. D. Stoll, pp. 131-140, Kluwer Academic Publishers, Netherlands, 1991.
- Press, W.H., Teukolsky, S.A., Vetterling, W.T. & Flannery B.P., Numerical Recipes in C, Cambridge University Press, Cambridge, 1992
- Rea, J., Ground Penetrating Radar Applications in Hydrology, Ph.D. dissertation, University of British Columbia, 88 pages, 1996.

- Rea, J., and Knight, R.J., The use of ground penetrating radar for aquifer characterization: an example from southwestern British Columbia, Proceedings, Symposium for Application of Geophysics to Environmental and Engineering Problems, 23-26 April, Orlando, FL, 10 pages, 1995.
- Rea, J., and Knight, R., Obtaining estimates of electrical conductivity from the attenuation in ground penetrating radar data, submitted to Geophysics September 1997, in revision.
- Rea, J., and Knight, R., Geostatistical analysis of ground penetrating radar data: A means of describing spatial variation in the subsurface, *Water Resources Research*, 34, 329-339, 1998.
- SCION Image, Copyright 1997 Scion Corporation
- Smith, D. G and Jol, H. M., Ground-penetrating radar investigation of a Lake Bonneville delta, Provo level, Brigham City, Utah, *Geology*, 20, 1083-1086, 1992a.
- Smith, D. G. and Jol, H. M., GPR results used to infer depositional processes of coastal spits in large lakes. Geological Survey of Finland, Special Paper 16, 169-177, 1992b.
- Ward, S. H., Hohmann, G. W., 1994, Electromagnetic Theory for Geophysics Applications, in Nabighian, M. N. Ed., *Electromagnetic Methods in Applied Geophysics: Investigations in Geophysics*, Society of Exploration Geophysicists, 1, 131-311.